Peptide-based probes for protein N-Methyltransferases

Zhang, Y.

Supplementary materials for Chapter 2-5
Appendix I - IV

Appendix I Supplementary materials for Chapter 2

High resolution Mass Spectrometry (HRMS) data for compounds 1-6:

1: HRMS (m/z): $[M+H]^+$ calculated for $C_{35}H_{60}N_{17}O_{11}^+$, 894.4653, found 894.4670.

2: HRMS (m/z): $[M+H]^+$ calculated for $C_{37}H_{62}N_{17}O_{12}^+$, 936.4758, found 936.4782.

3: HRMS (m/z): $[M+H]^+$ calculated for $C_{41}H_{72}N_{19}O_{12}^+$, 1022.5602, found 1022.5621.

4: HRMS (m/z): $[M+H]^+$ calculated for $C_{43}H_{74}N_{19}O_{13}^+$, 1064.5708, found 1064.5730.

5: HRMS (m/z): $[M+H]^+$ calculated for $C_{25}H_{48}N_{12}O_8^+$, 645.3796, found 645.3795.

6: HRMS (m/z): $[M+H]^+$ calculated for $C_{31}H_{60}N_{14}O_9^+$, 773.4746, found 773.4759.

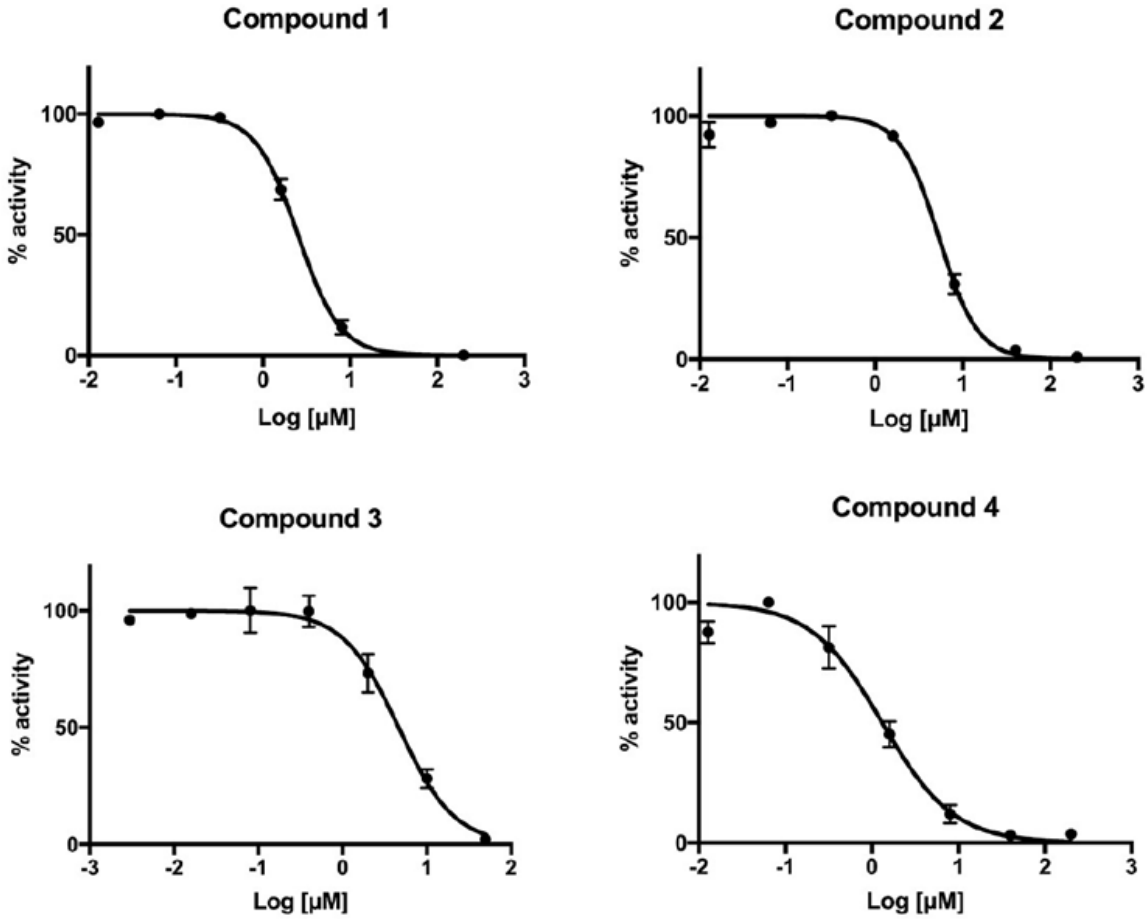

Figure S1a. IC_{50} curves for compounds 1-4 against PRMT1

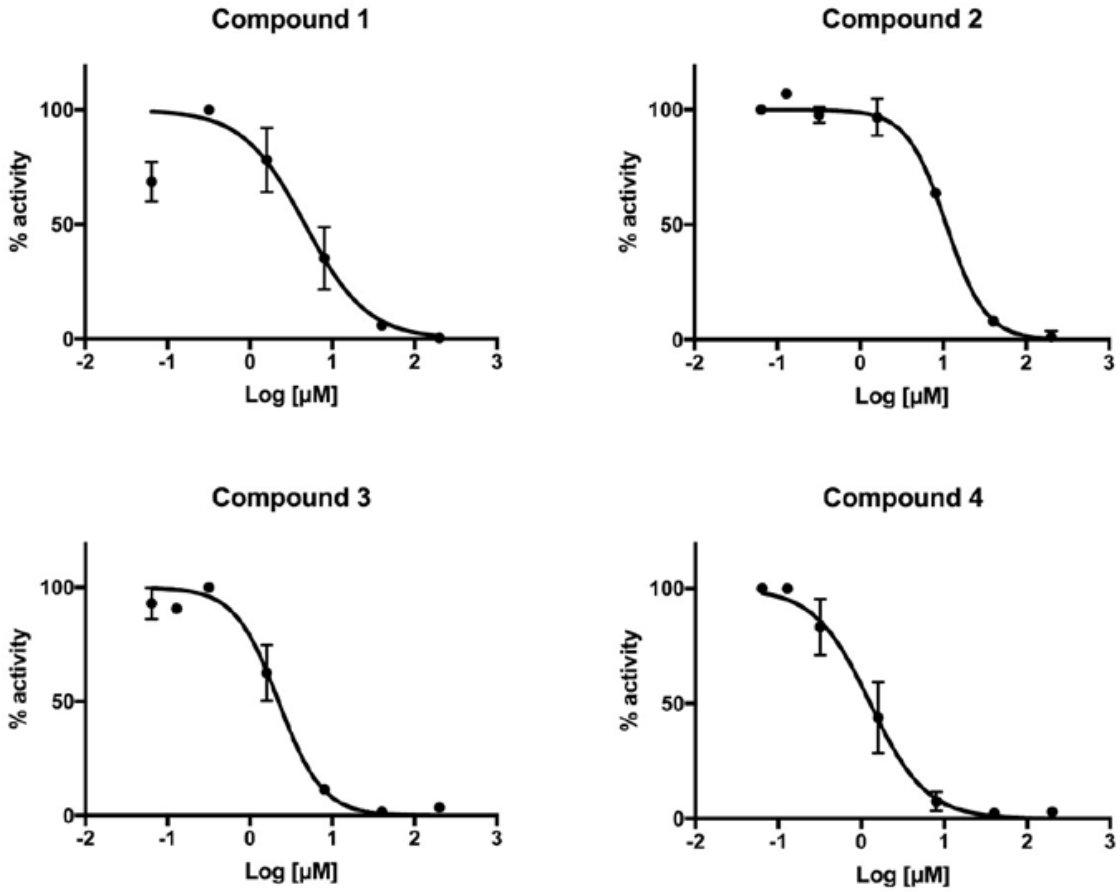

Figure S1b. IC_{50} curves for compounds 1-4 against PRMT6

HPLC traces of final compounds

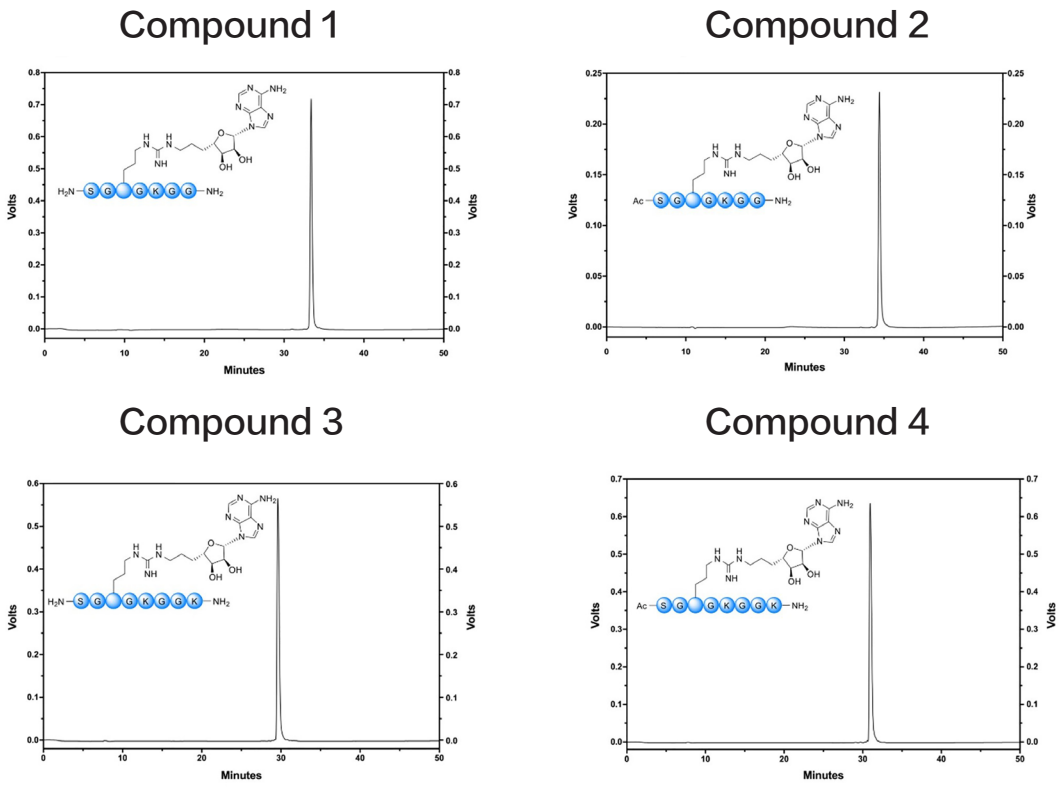

Compound 3

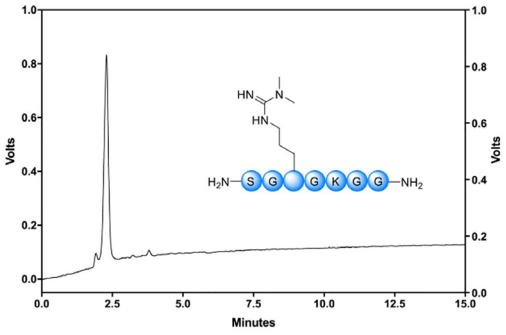

Compound 4

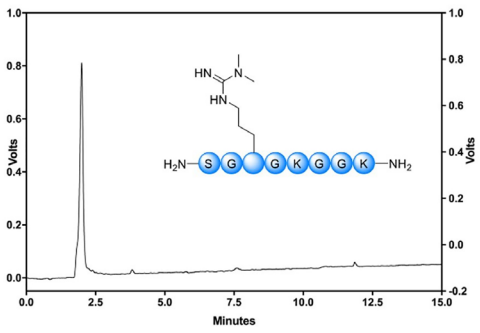

A

Appendix II Supplementary materials for Chapter 3

High Resolution Mass Spectrometry data and purified yields of compounds 1-14

Table S1. High Resolution Mass Spectrometry data and purified yields of compounds 1-14

Compound	Chemical formula	Calculated Mass	Found	Yield
1	$C_{201}H_{347}N_{74}O_{55}^{3+}$	1559.2205	1559.2210	11%
2	$C_{203}H_{350}N_{74}O_{56}^{4+}$	1180.1698	1180.1703	8%
3	$C_{98}H_{170}N_{36}O_{26}^{2+}$	1134.1555	1134.1544	23%
4	$C_{100}H_{172}N_{36}O_{27}^{2+}$	1155.1608	1155.1606	26%
5	$C_{81}H_{141}N_{29}O_{24}^{2+}$	952.0297	952.0274	40%
6	$C_{83}H_{143}N_{19}O_{13}^{2+}$	973.0349	973.0330	39%
7	$C_{60}H_{103}N_{22}O_{16}^{+}$	1387.7922	1387.7912	47%
8	$C_{62}H_{105}N_{22}O_{17}^{+}$	1429.8082	1429.8052	41%
9	$C_{54}H_{93}N_{20}O_{13}^{+}$	1229.7231	1229.7223	50%
10	$C_{56}H_{95}N_{20}O_{14}^{+}$	1271.7336	1271.7340	50%
11	$C_{45}H_{76}N_{17}O_{11}^{+}$	1030.5910	1030.5907	51%
12	$C_{47}H_{78}N_{17}O_{12}^{+}$	1072.6070	1072.6012	50%
13	$C_{36}H_{60}N_{15}O_{9}^{+}$	846.4698	846.4697	53%
14	$C_{38}H_{62}N_{15}O_{10}^{+}$	888.4804	888.4812	55%

HPLC traces of compounds 1-14

HPLC chromatograms of compounds 1-4 were obtained by analytical RP-HPLC using a Phenomenex Kinetex C18 column (250 × 4.6 mm, 5 μm particle size) with UV detection at 214 nm. The following solvent system, at a flow rate of 0.7 mL/min, was used: solvent A, 0.1 % formic acid in water; solvent B, methanol. Gradient elution was as follows: 95:5 (A/B) for 5 min, 95:5 to 50:50 (A/B) over 15 min, then reversion back to 95:5 (A/B) over 1 min, 95:5 (A/B) for 4 min.

HPLC chromatograms of compounds 5-14 were obtained by LCMS using a Shimadzu Shim-Pack GIST-AQ C18 column (3.0 x 150 mm, 3 μm particle size) with UV detection at 214 nm. The following solvent system, at a flow rate of 0.5 mL/min, was used: solvent A, 0.1 % formic acid in water; solvent B, acetonitrile. Gradient elution was as follows: 95:5 (A/B) for 2 min, 95:5 to 0:100 (A/B) over 23 min, 0:100 (A/B) for 1 min, then reversion back to 95:5 (A/B) over 1 min, 95:5 (A/B) for 3 min.

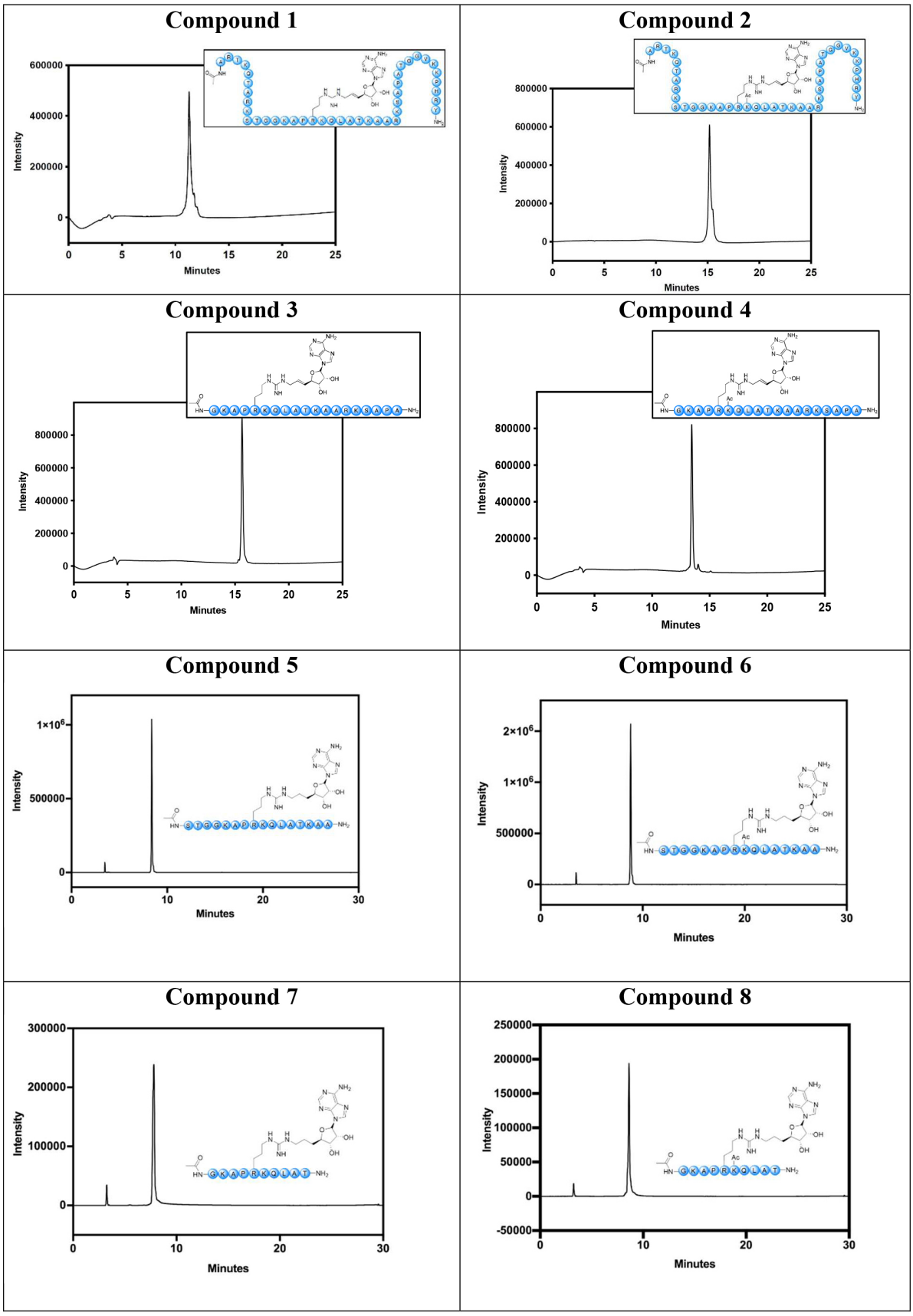
Compound 1
Intensity
Minutes
Compound 2
Intensity
Minutes
Compound 3
Intensity
Minutes
Compound 4
Intensity
Minutes
Compound 5
Intensity
Minutes
Compound 6
Intensity
Minutes
Compound 7
Intensity
Minutes
Compound 8
Intensity
Minutes

Compound 9

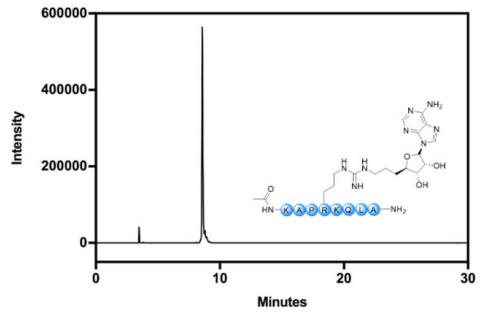

Compound 10

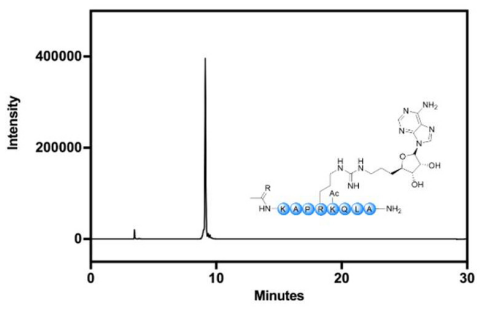

Compound 11

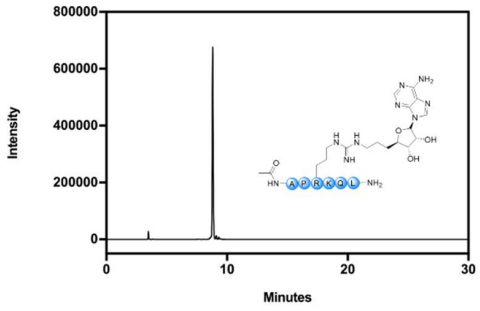

Compound 12

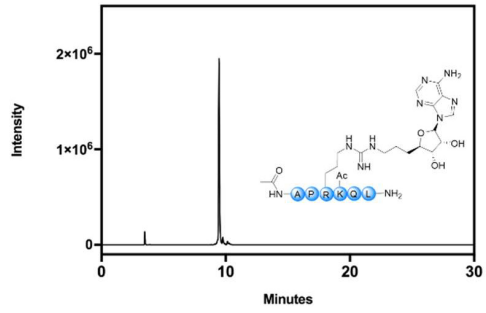

Compound 13

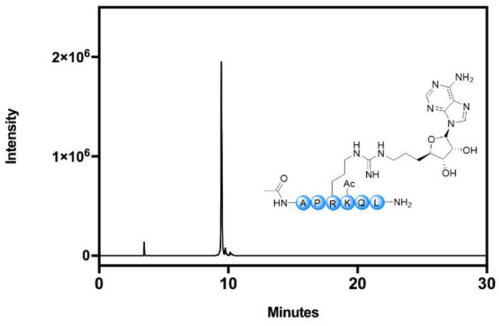

Compound 14

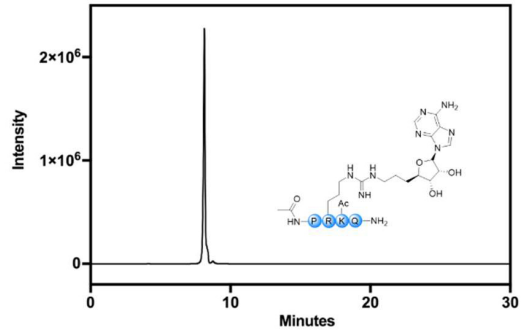

A

IC_{50} curves for compounds 5-14 and SAH

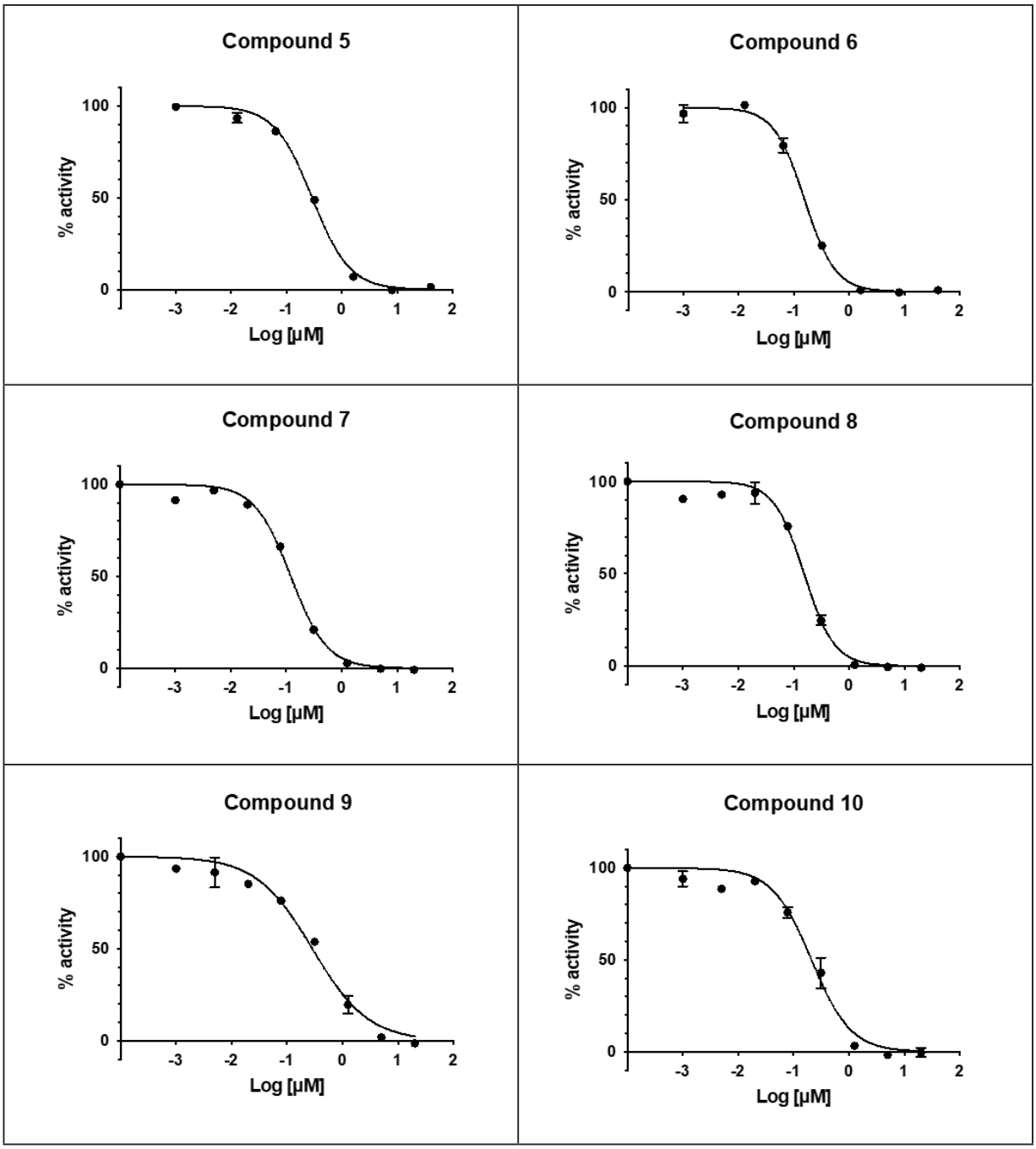

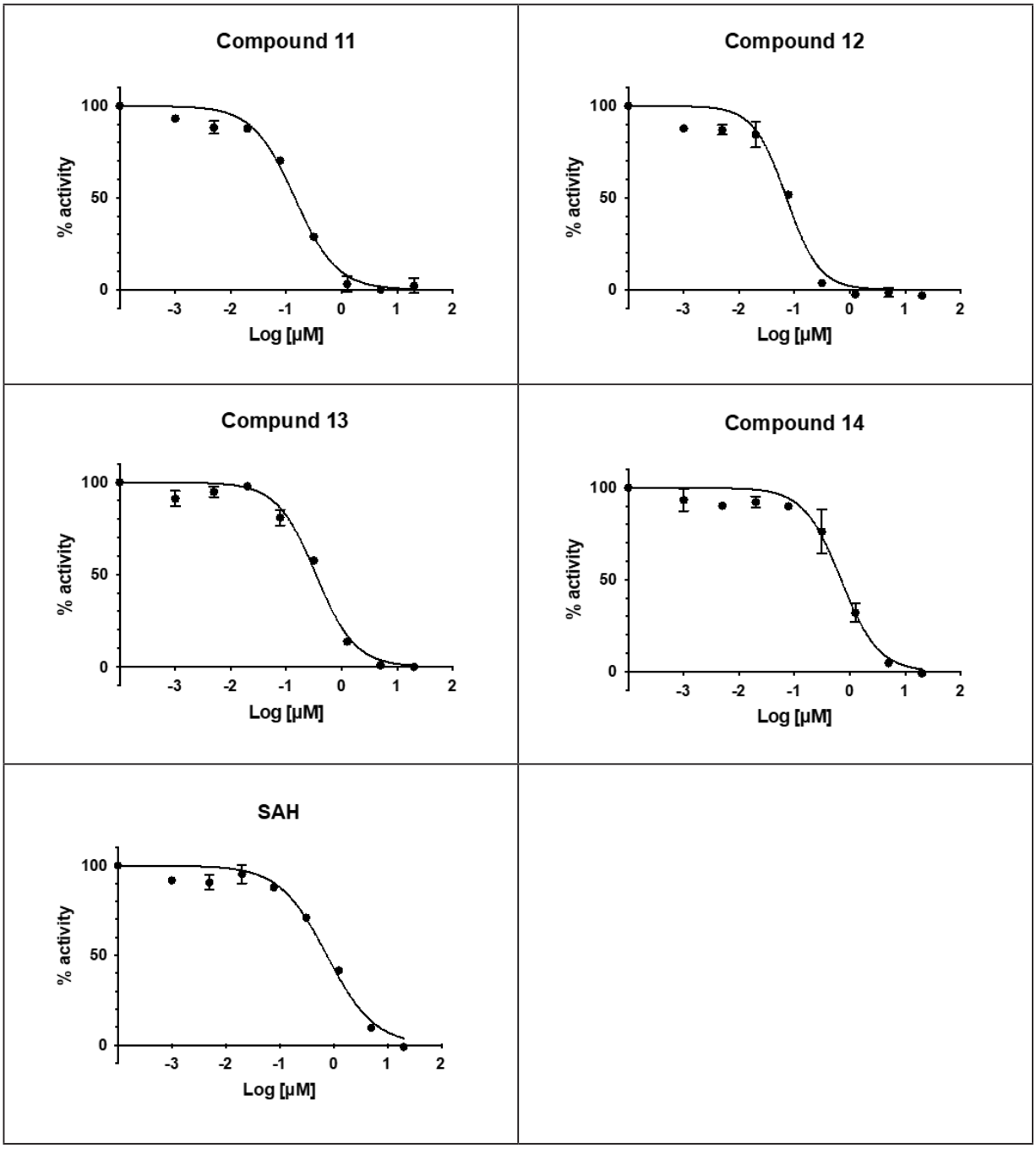
Compound 11
% activity
100
50
0
-3
-2
-1
0
1
2
Log [µM]
Compound 12
% activity
100
50
0
-3
-2
-1
0
1
2
Log [µM]
Compund 13
% activity
100
50
0
-3
-2
-1
0
1
2
Log [µM]
Compound 14
% activity
100
50
0
-3
-2
-1
0
1
2
Log [µM]
SAH
% activity
100
50
0
-3
-2
-1
0
1
2
Log [µM]

Comparative table of IC_{50} values and Ki values for compounds 5-14 and SAH

IC_{50} values were determined as described in the experimental section. Briefly, normalized luminescence data from the activity assay was plotted as a function of inhibitor concentration and analyzed using the following equation:

$$Y = \frac{100}{(1 + 10^{((logIC50 - X) \times Hill\ Slope)})}$$

Where Y = percentage activity, X = the logarithmic concentration of the inhibitors, Hill Slope= slope factor or Hill coefficient. The IC_{50} value was determined by the half maximal inhibitory concentration. The IC_{50} values measured for SAH, which served as a reference compound, are similar to those reported.

The K_I values were determined using the same normalized luminescence data from the activity assay using the following equation:

$$Y = Vo * (1 - \frac{\left(Et + X + \left(Ki * \left(1 + \left(\frac{S}{Km}\right)\right)\right)\right) - \sqrt{((Et + X + \left(Ki * \left(1 + \left(\frac{S}{Km}\right)\right)\right))^2 - 4 * Et * X)}}{(2 * Et)})$$

Where Y = percentage activity, X = Concentration of inhibitor, Et = Enzyme concentration in micromolar, KM: Michealis-Menten constant of enzyme, KI: Dissociation constant of inhibitor in micromolar. Equation 9.6, in R.A. Copeland, Enzymes, 2nd edition, Wiley, 2001.

The enzyme concentration was fixed at 0.2 μM and the substrate concentration was 12 μM for the PABP1 peptide, which is equal to its KM value.

Table S2. IC_{50} values and Ki values for compounds 5-14

Compound		CARM1 Inhibition (μM)[a]	
		IC_{50}	K_I
SAH		0.756 ± 0.089	0.391 ± 0.040
5	$H3^{10-25}$	0.290 ± 0.015	0.096 ± 0.009
6	$H3^{10-25}(K^{18}Ac)$	0.155 ± 0.007	0.028 ± 0.004
7	$H3^{13-22}$	0.121 ± 0.007	0.020 ± 0.002
8	$H3^{13-22}(K^{18}Ac)$	0.155 ± 0.012	0.030 ± 0.005
9	$H3^{14-21}$	0.287 ± 0.034	0.137 ± 0.018
10	$H3^{14-21}(K^{18}Ac)$	0.211 ± 0.023	0.066 ± 0.011
11	$H3^{15-20}$	0.143 ± 0.014	0.036 ± 0.005
12	$H3^{15-20}(K^{18}Ac)$	0.072 ± 0.008	0.001 ± 0.002
13	$H3^{16-19}$	0.346 ± 0.031	0.130 ± 0.017
14	$H3^{16-19}(K^{18}Ac)$	0.699 ± 0.081	0.320 ± 0.051

[a] IC_{50} and KI values reported in μM from duplicate data obtained from a minimum of 7 different concentrations ± standard error of the mean (s.e.m.).

Supplemental table and figures for structural studies

Table S3. X-ray data collection and refinement statistics for mmCARM1 complexes with H313-31 peptidomimetics 3 and 4

PDB ID		7OKP	7OS4
TS Mimic		H313-31 K18Ac	H313-31 K18
Data processing	Resolution (Å)	46.11-2.20 (2.25-2.20)	45.76-2.54 (2.62-2.54)
	space group	P21212	P21212
	cell	74.91 99.58 208.07	74.37 98.61 206.61
	Total reflections	406216 (16351)	315674 (22239)
	Unique reflections	77281 (4317)	49843 (4042)
	Rmerge	0.092 (0.693)	0.129 (2.284)
	Rmeas	0.101 (0.809)	0.140 (2.501)
	Rpim	0.040 (0.406)	0.055 (0.996)
	I/σI	9.3 (1.5)	8.6 (0.6)
	CC1/2	0.998 (0.690)	0.999 (0.475)
	Completeness (%)	97.1 (93.7)	97.9 (87.4)
	Multiplicity	5.3 (3.8)	6.3 (5.5)
	Wilson B ($Å^2$)	35.2	63.5
	Resolution limit for I//σ (I) > 2.0 (A)	2.36	2.96
Refinement	Resolution (Å)	45.32 – 2.2 (2.28 - 2.2)	45.76 - 2.542 (2.632 - 2.54)
	Rwork (%)	21.08 (31.08)	0.71 (35.19)
	Rfree (%	25.45 (34.88)	25.94 (36.78)
	Number of non-hydrogen atoms	12185	11675
	macromolecules	11589	11504
	ligands	297	266
	solvent	425	21
Validation	RMS(bonds)	0.003	0.003
	RMS(angles)	0.59	0.54
	Ramachandran favored (%)	95.64	95.49
	Ramachandran outliers (%)	0.00	0.00
	Rotamer outliers (%)	0.32	2.00
	Average B-factor	47.62	64.83

Statistics for the highest-resolution shell are shown in parentheses. The resolution limits for I/ σ (I) > 2 are reported.

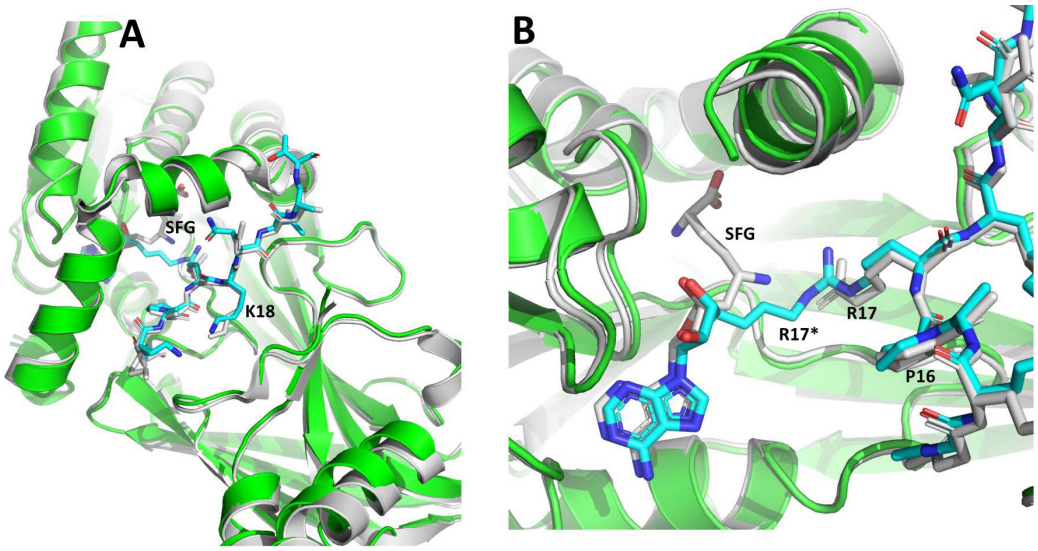

Figure S1. Structure of transition state mimic overlaid with isolated peptide in presence of SFG. (A) $H3^{13-31}$ K^{18} peptidomimetic 3 in complex with mmCARM1 (green cartoon and blue sticks, PDB code 7OS4) superimposed with structure of SFG-H3R17 bound to hs-CARM1 (gray cartoon/sticks, PDB code 5DX0). (B) Close-up around the SFG binding site. For clarity, the N-terminal helices of mmCARM1 and hsCARM1 are not shown.

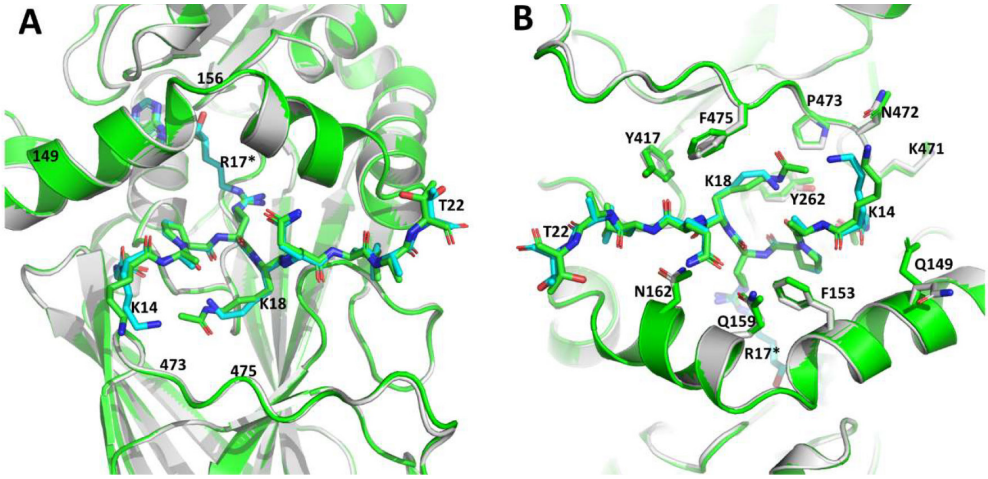

Figure S2. Superimposition of $H3^{13-31}(Lys^{18}NH_2)$ and $H3^{13-31}(Lys^{18}Ac)$ complexes with mmCARM1 (only local view of monomer A shown). (A) Superposition of $H3^{13-31}(Lys^{18}NH_2)$ (blue sticks) and $H3^{13-31}(Lys^{18}Ac)$ (green sticks) bound to mmCARM1 (gray/green cartoon) (monomer A), PDB codes 7OS4 and 7OKP respectively. (B) Close-up view of recognition mode for $H3^{13-31}(Lys^{18}NH_2)$ and $H3^{13-31}(Lys^{18}Ac)$.

Appendix III Supplementary materials for Chapter 4

LC-MS traces of analyte and internal standard

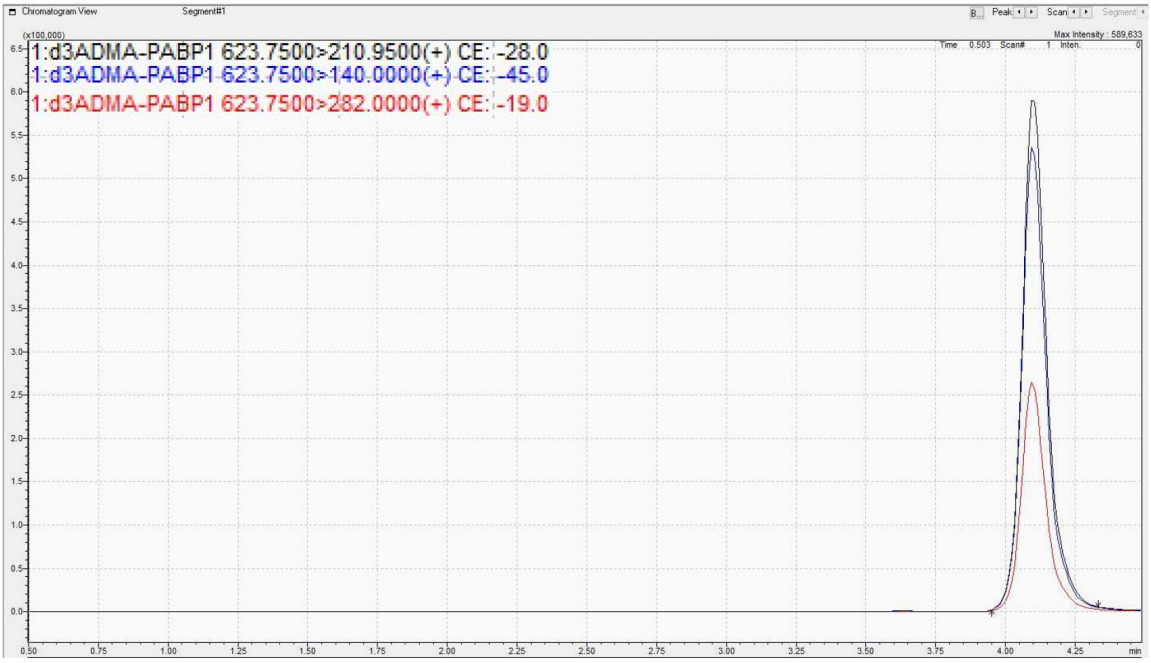

Figure S1. LC-MS/MS traces of PABP1$^{456\text{-}466}$R^{460}-d_6-aDMA (internal standard). MS method: 0.5-4.5 min; retention time 4.101 min, Q1 mass detection; 623.75; Q3 mass detection: 282.00, 210.95, 140.00.

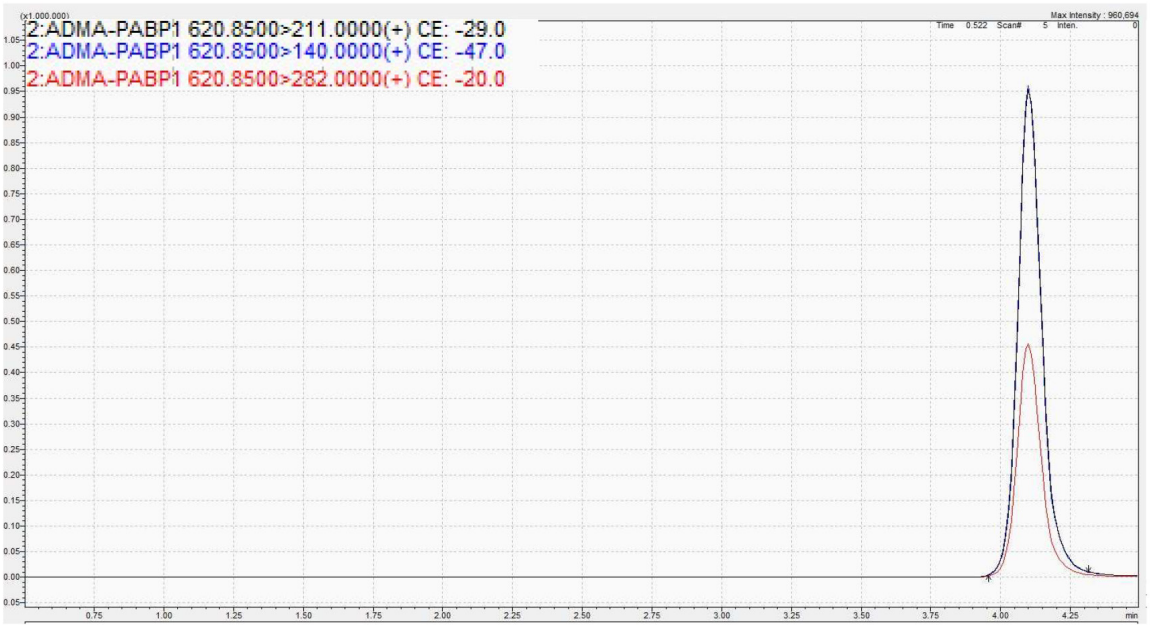

Figure S2. LC-MS/MS traces of PABP1$^{456\text{-}466}$ R^{460}-aDMA (methylated product). MS method: 0.5-4.5 min; retention time 4.101 min, Q1 mass detection; 620.85; Q3 mass detection: 282.00, 211.00, 140.00.

Kinetic analysis of CARM1 substrates

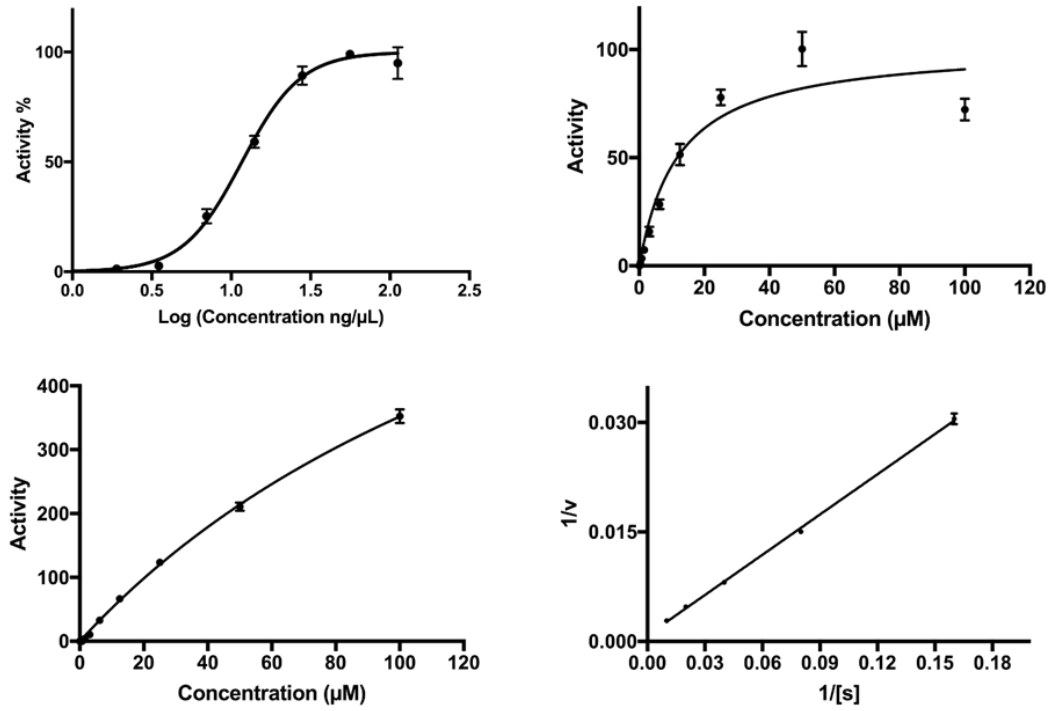

Figure S3. A. EC_{50} curve for CARM1, EC_{50} = 11.68 ± 0.33 ng/µL. B. Michaelis-Menten Plot for K_M value determination of $PABP1^{456-466}$, $K_{M,\ PABP1\ 456-466}$= 12.03 ± 2.28 µM. C. Michaelis-Menten Plot and Lineweaver Burk plot (D) for K_M value determination of AdoMet, $K_{M,\ AdoMet}$= 5.46 ± 0.01 µM.

A

IC50 curves for compounds 1-9

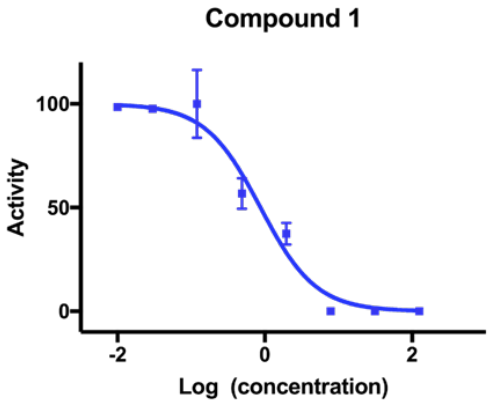

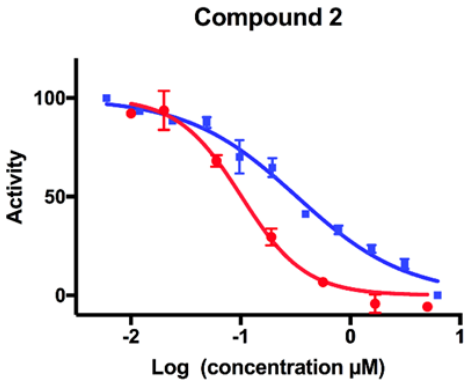

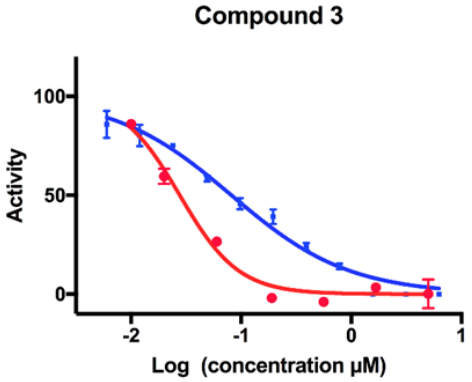

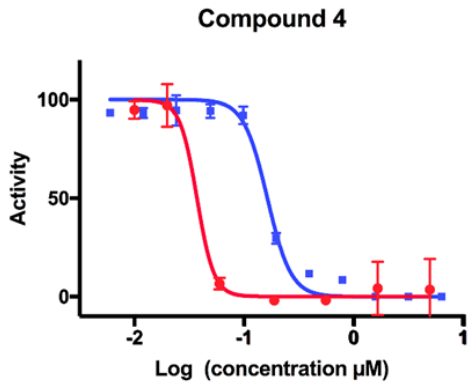

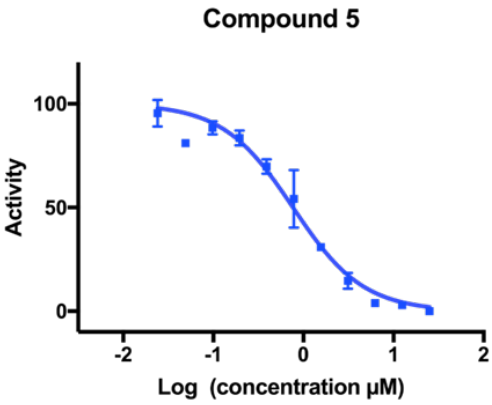

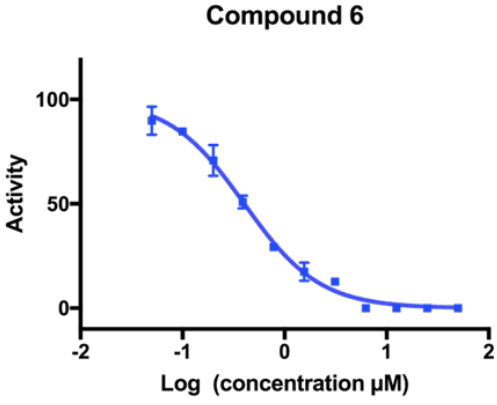

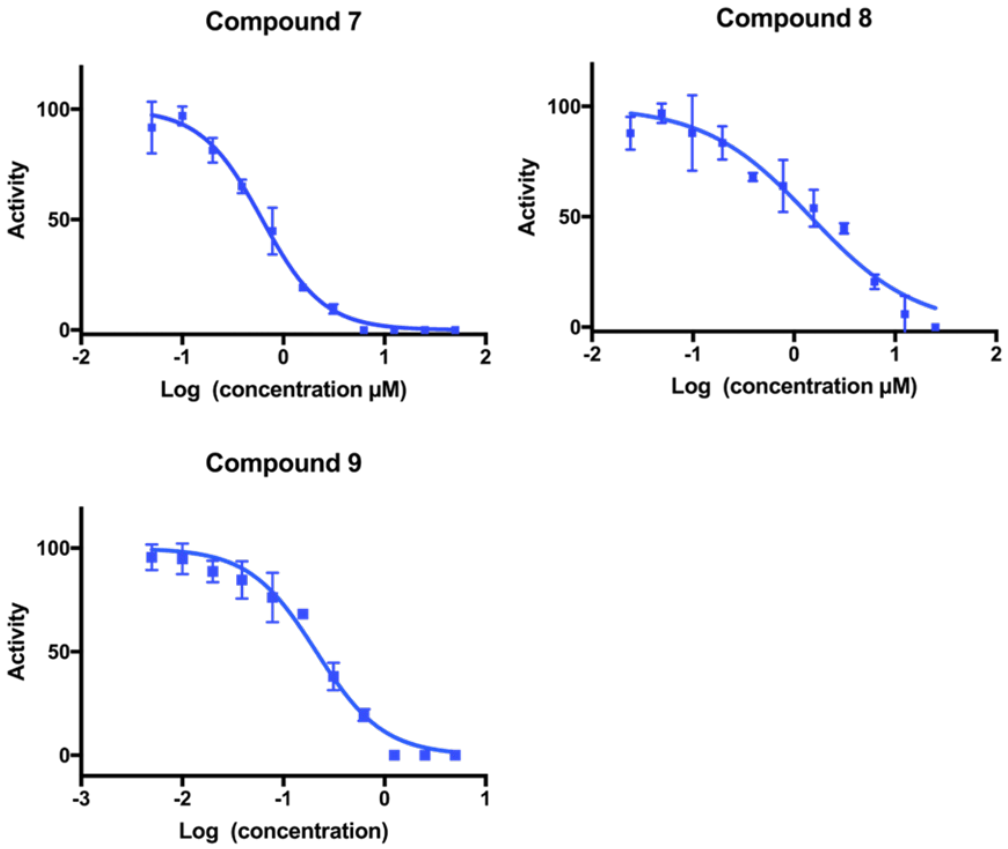

Figure S4. IC_{50} curves of inhibitors 1-9. Blue curves represent the measurements obtained using the MRM LC-MS assay and red curves correspond to measurements obtained using commercially available the ELISA assay kit. The ELISA assay based IC_{50} values for compounds 1, 5-9 presented in Table 3 of the manuscript are taken from our previously published work and the corresponding inhibition curves can be found there (refs 27 and 20).

A

HPLC and High Resolution Mass Spectrometry data for PABP1$^{456-466}$ peptides

High Resolution Mass Spectrometry (HRMS)

PABP1$^{456-466}$ (m/z):

$[M+H]^+$ calculated for $C_{55}H_{86}N_{15}O_{14}S^+$, 1212.6199, found 1212.6206.

PABP1$^{456-466}$R^{460}-aDMA (m/z):

$[M+H]^+$ calculated for $C_{57}H_{90}N_{15}O_{14}S^+$, 1240.6512, found 1240.6516.

PABP1$^{456-466}$R^{460}-d_6-aDMA (m/z):

$[M+H]^+$ calculated for $C_{57}H_{84}D_6N_{15}O_{14}S^+$, 1246.6889, found 1246.6894

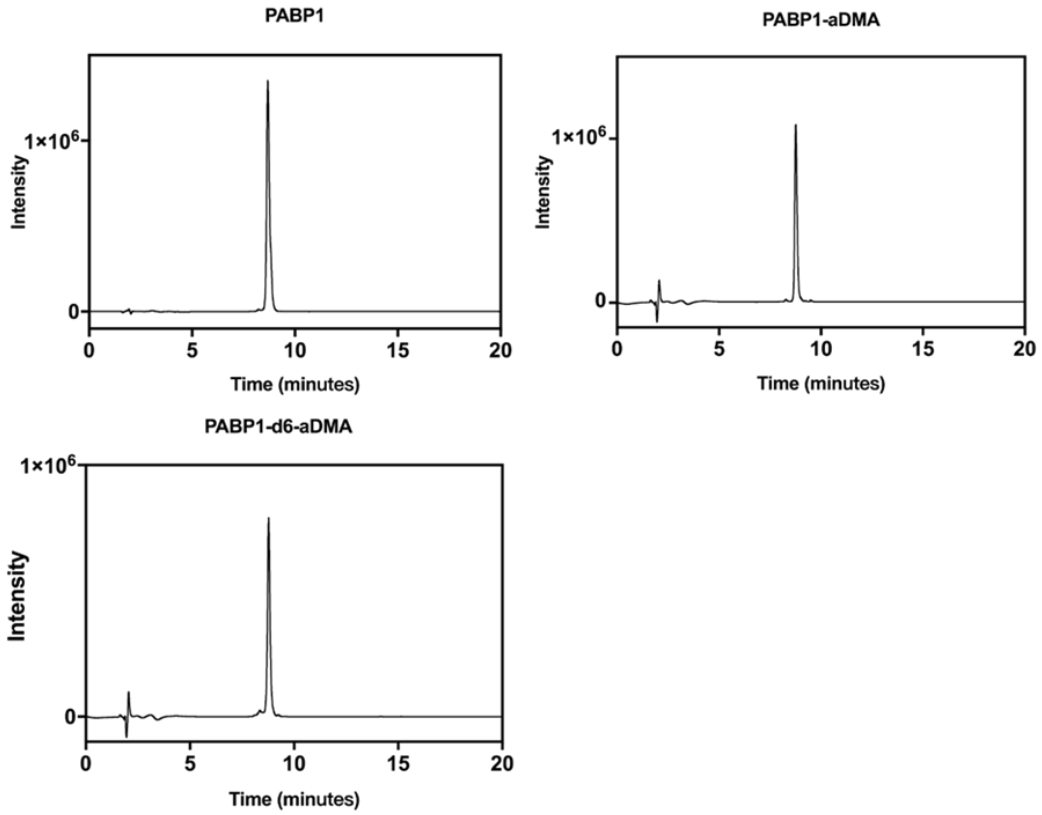

NMR Data of Fmoc-d_6-aDMA-OH

^{1}H NMR (500 MHz, $CDCl_3$)

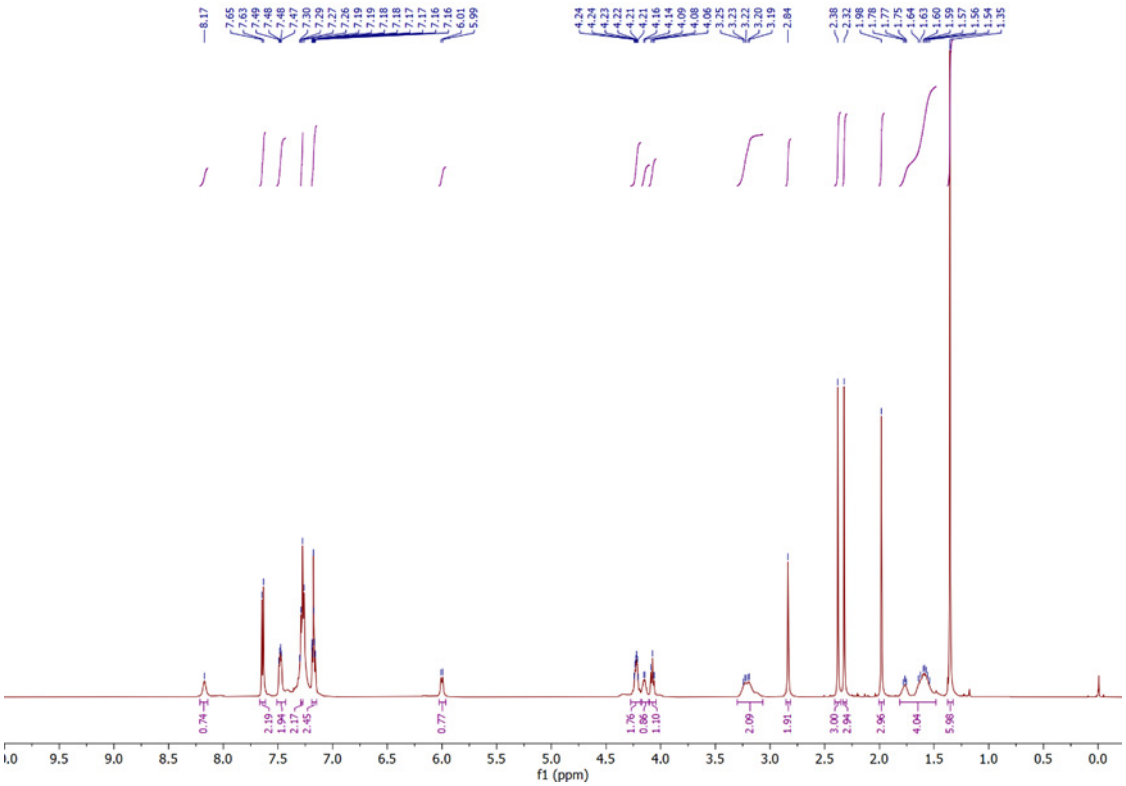

A

^{13}C NMR (126 MHz, $CDCl_3$)

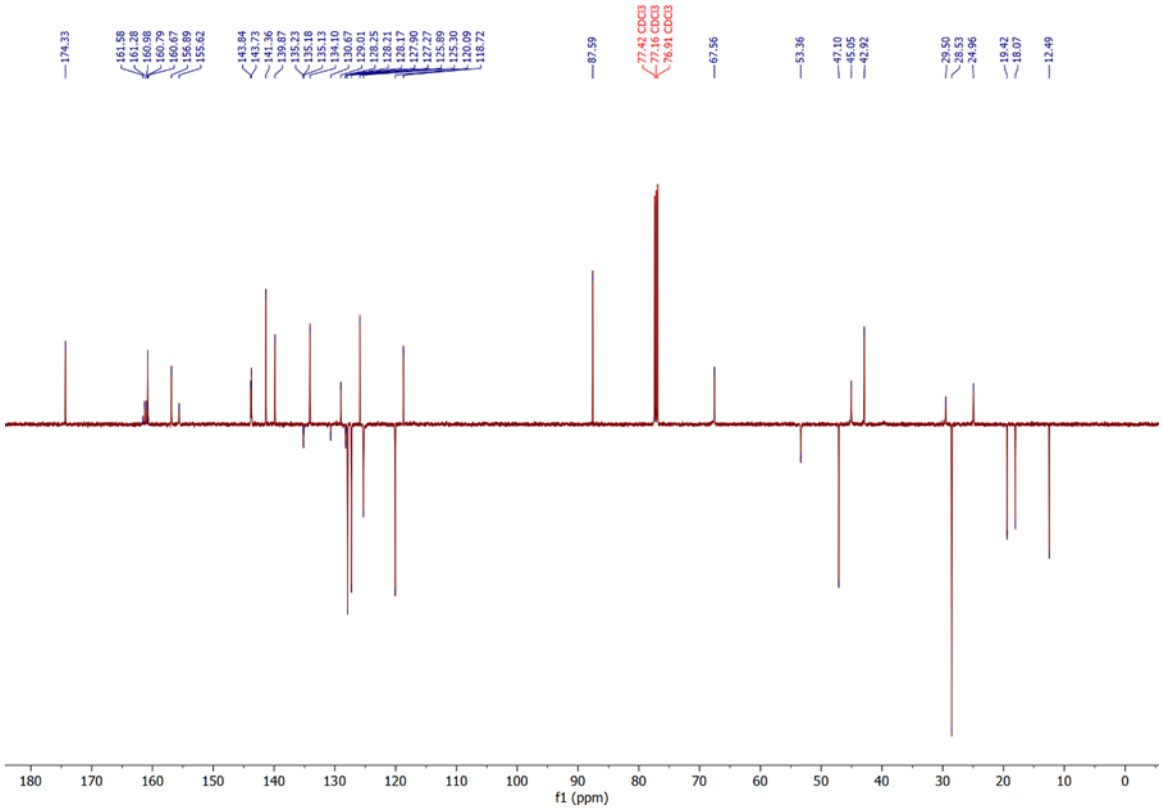

A

Appendix IV Supplementary materials for Chapter 5

Reprogrammed mRNA display protocol

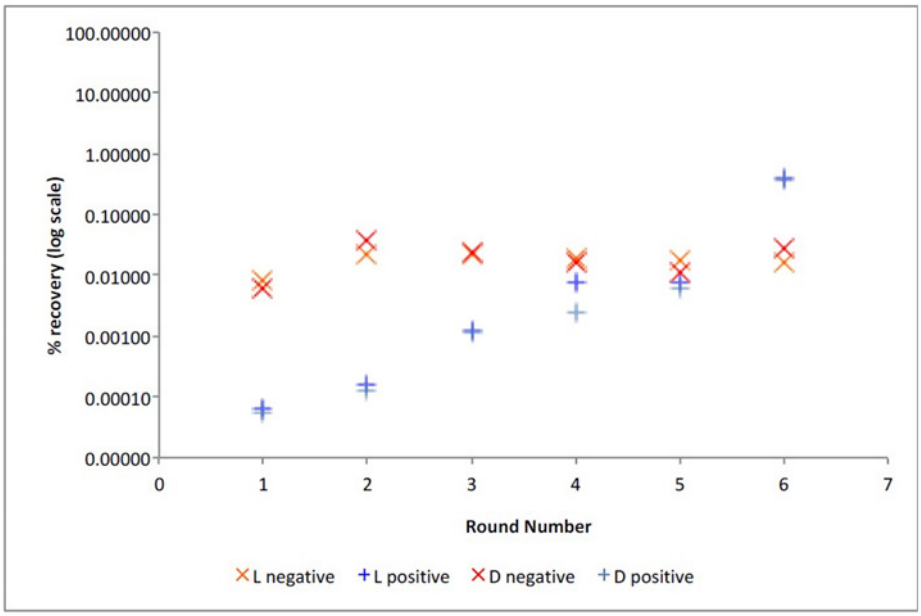

Figure S1. Library enrichment by binding to NNMT plotted across all selection rounds (log scale on Y-axis), showing binding against both immobilised NNMT ('positive', blue/light blue plus symbol) and against the immobilisation medium alone ('negative', orange/red cross symbol) for both the L- and D-tyrosine initiated libraries (respectively).

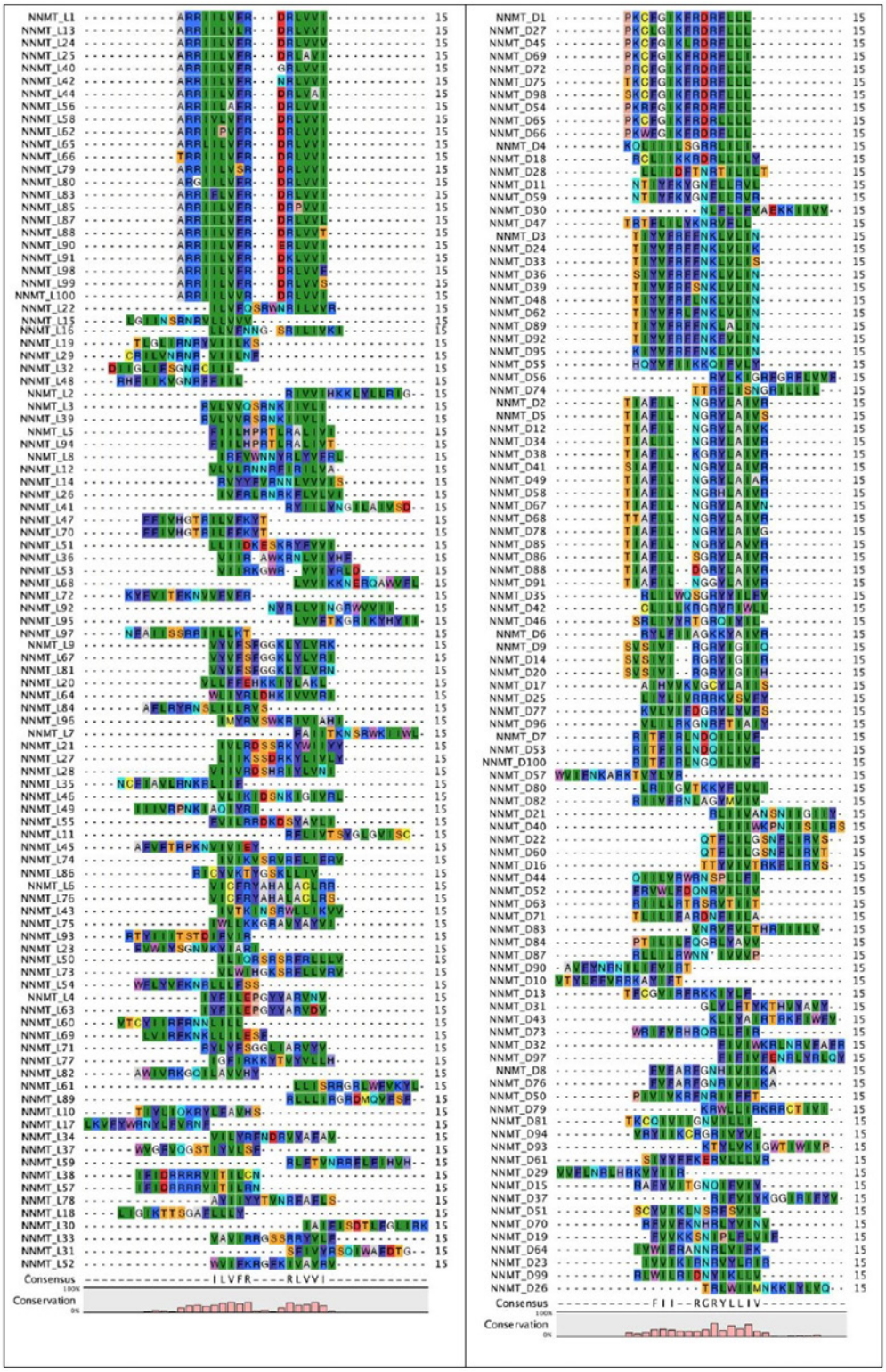

Figure S2. Sequence alignment of the L-tyrosine library (left) and D-tyrosine library (right). Colors indicate the properties of the respective amino acids. In both libraries hydrophobic (green) and positively charged (blue) amino acids are enriched.

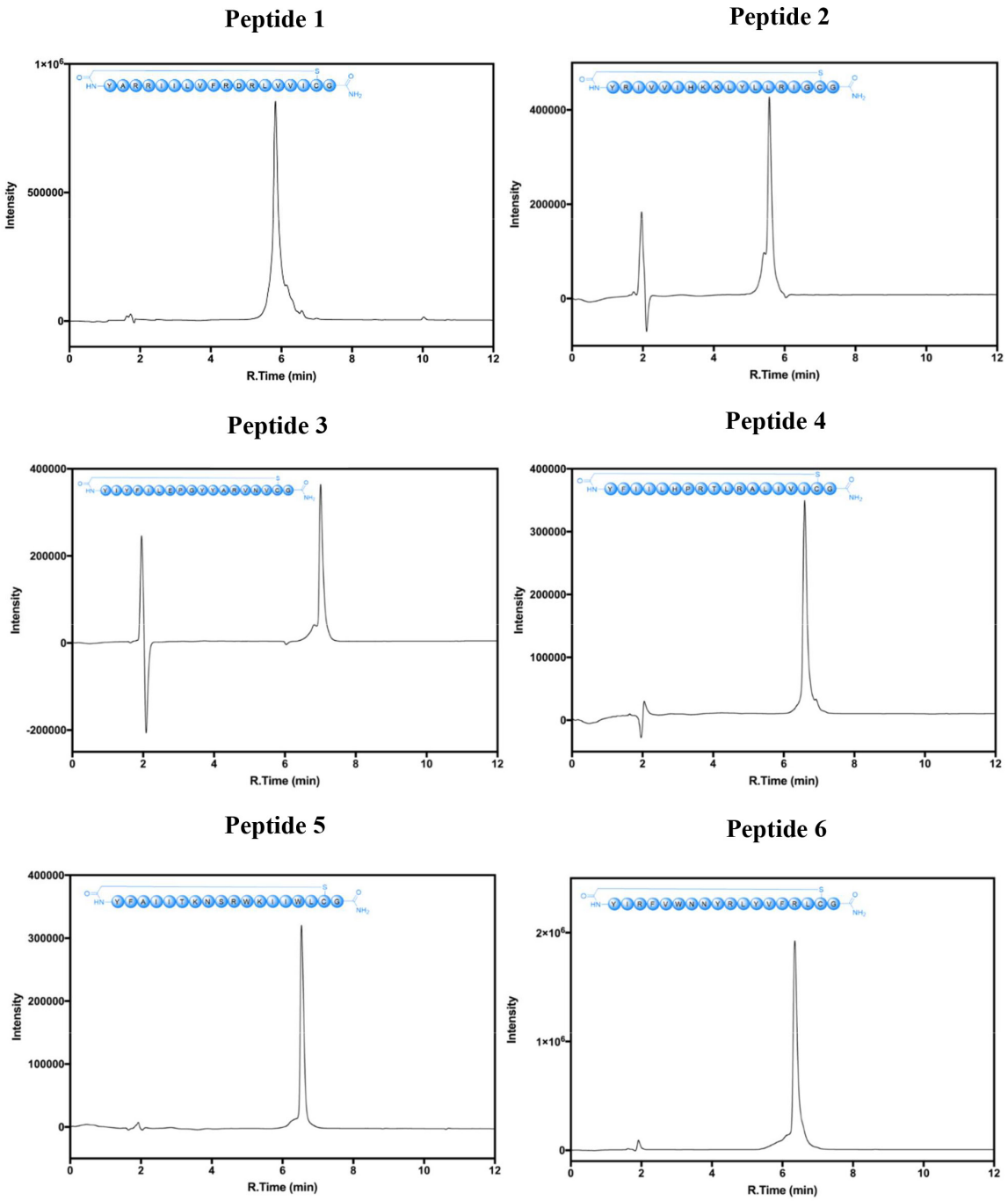

Figure S3. HPLC purity traces for peptides 1-6 over 12 minutes (5-100% acetonitrile).

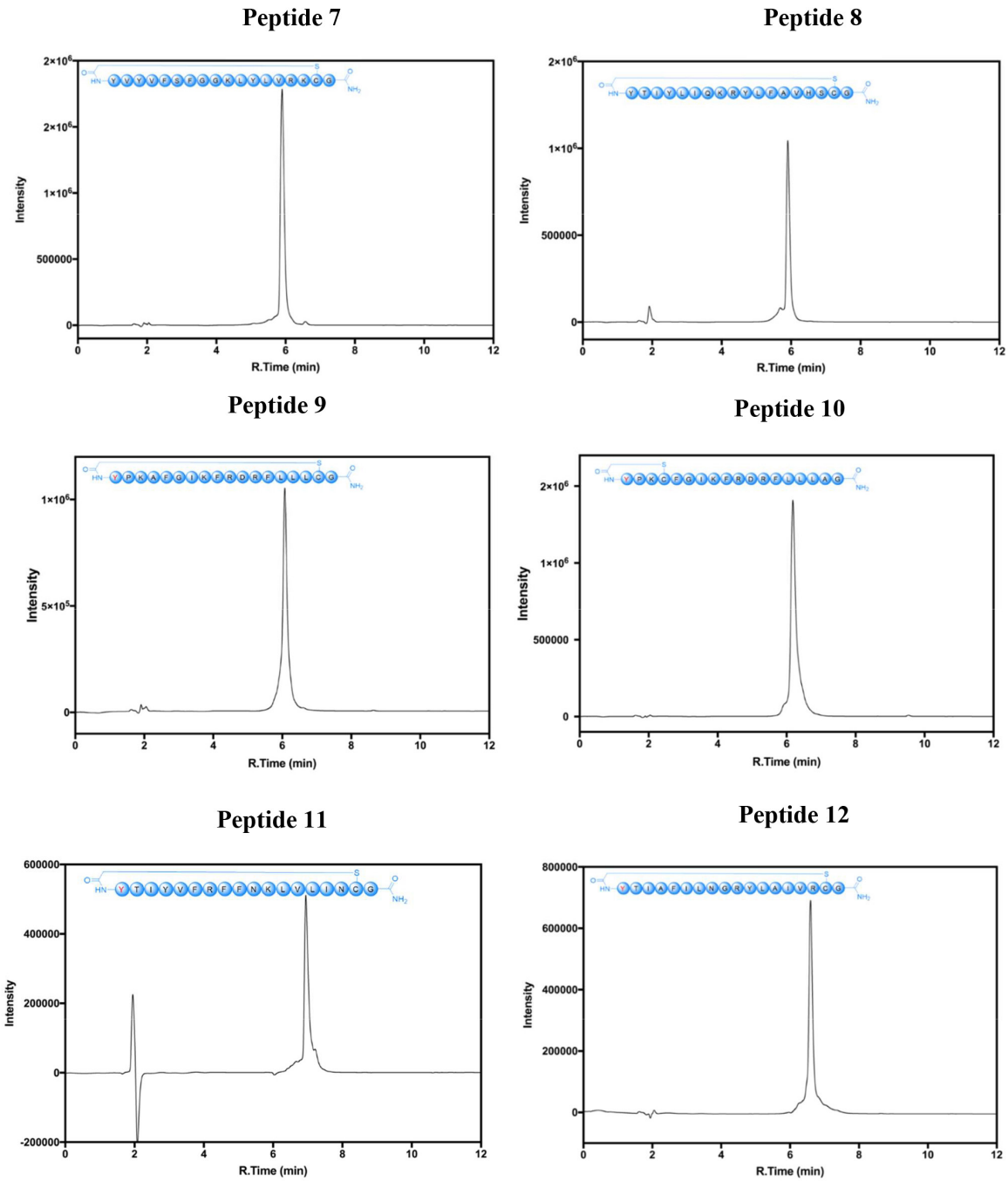

Figure S4. HPLC purity traces for peptides 7-12 over 12 minutes (5-100% acetonitrile).

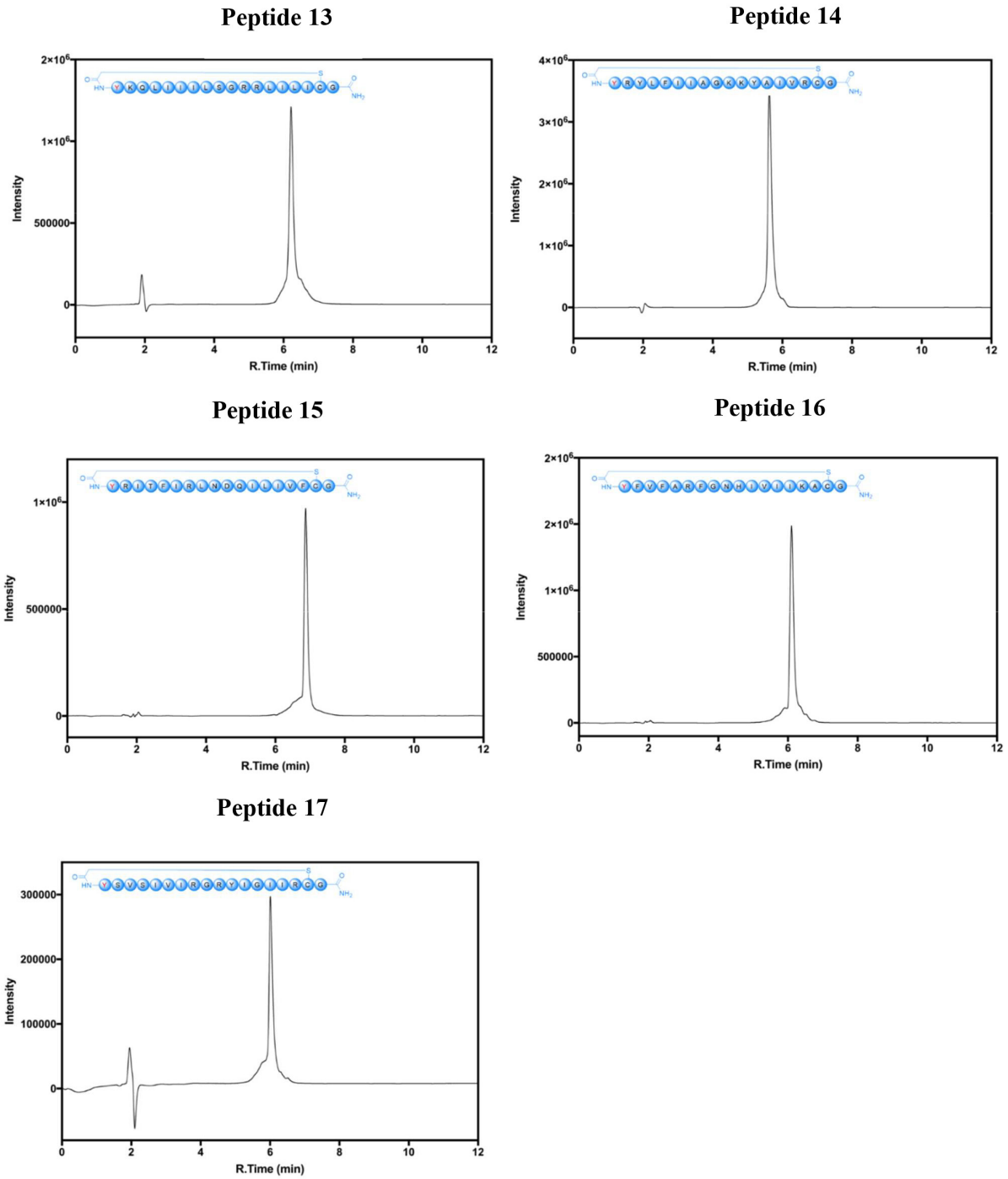

Figure S5. HPLC purity traces for peptides 13-17 over 12 minutes (5-100% acetonitrile).

IC_{50} curves

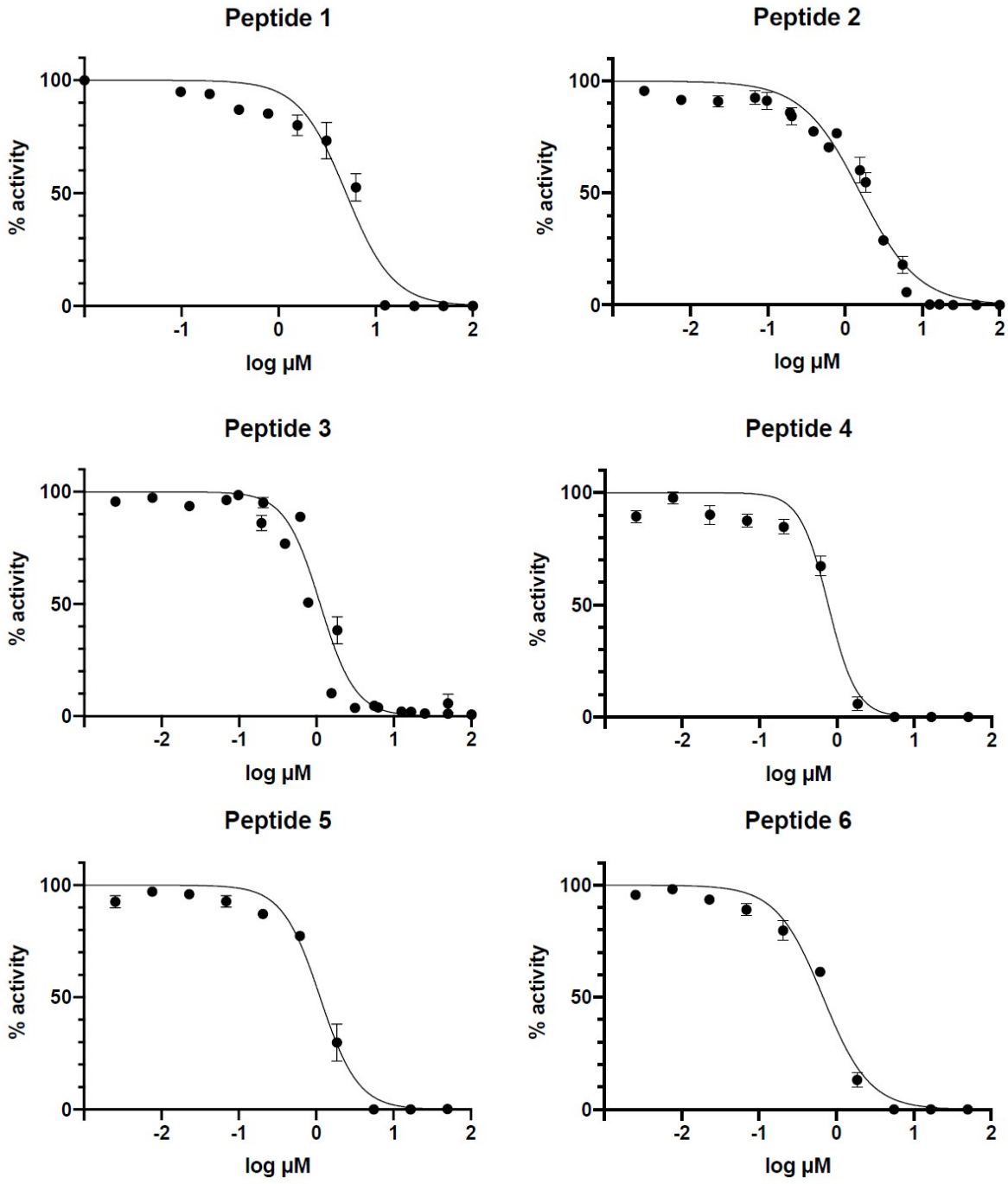

Figure S6. IC_{50} curves for peptides 1-6 against hNNMT. Data is based on triplicate data of at least 10 different concentrations

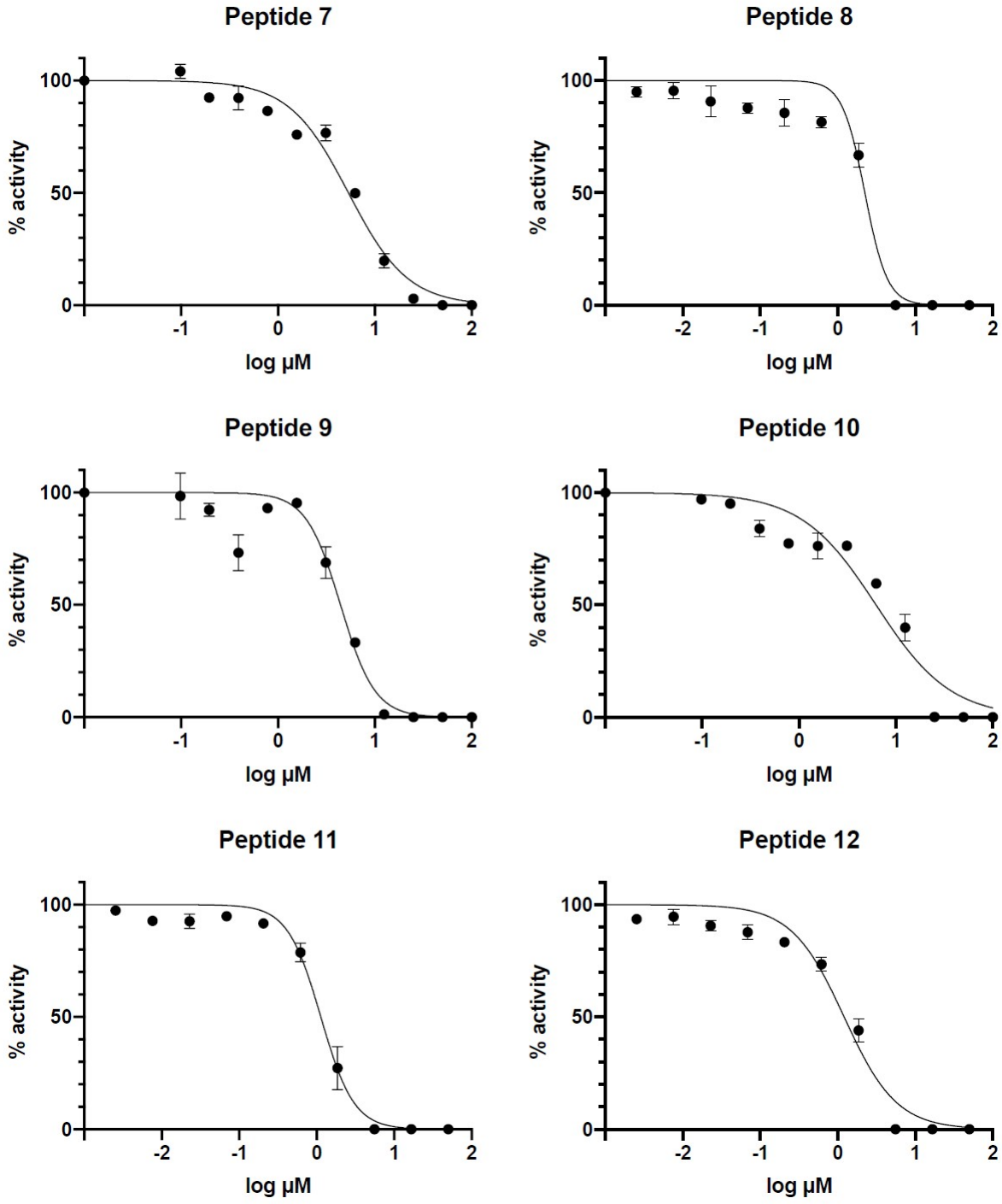

Figure S7. IC_{50} curves for peptides 7-12 against hNNMT. Data is based on triplicate data of at least 10 different concentrations

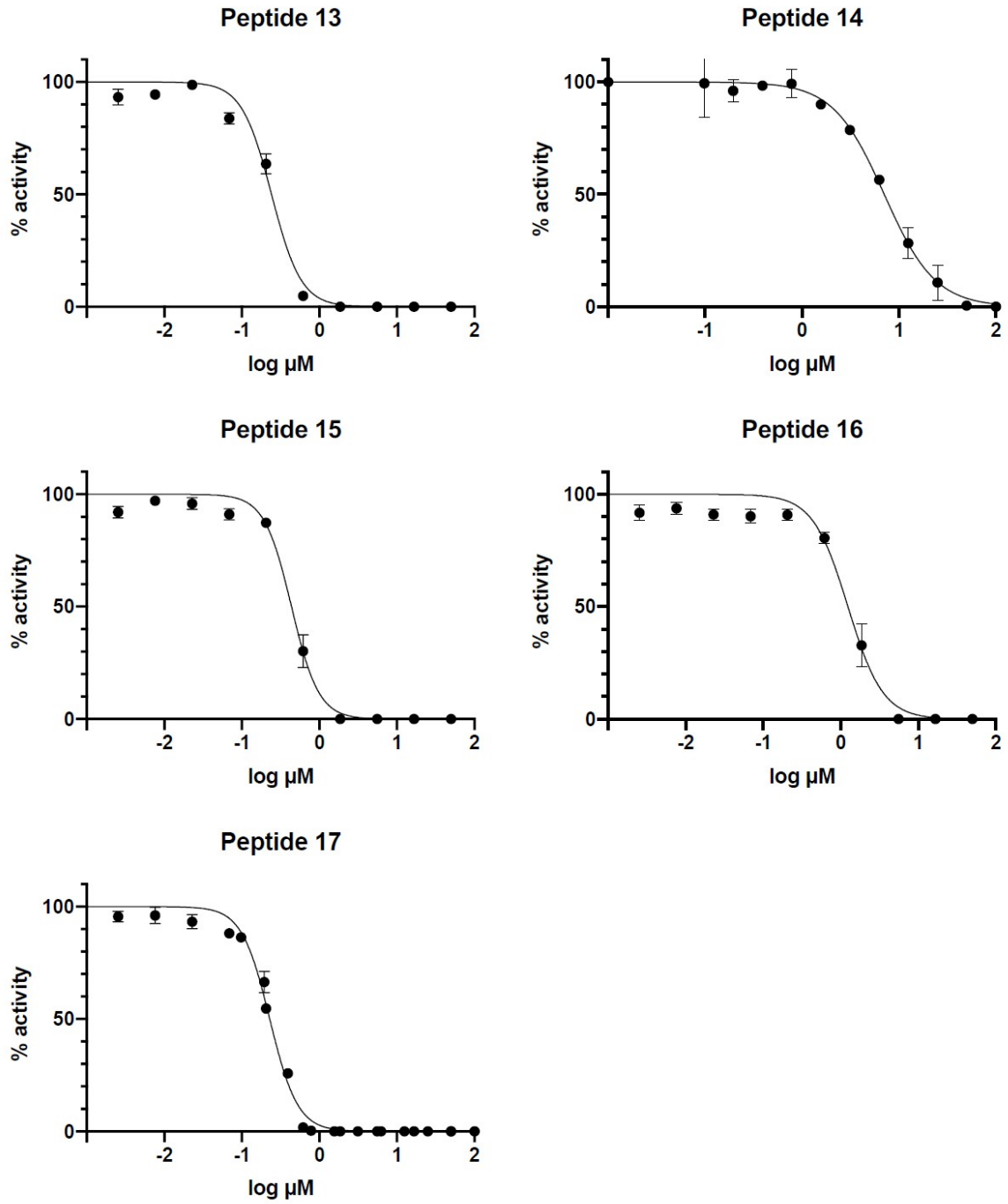

Figure S8. IC_{50} curves for peptides 13-17 against hNNMT. Data is based on triplicate data of at least 10 different concentrations

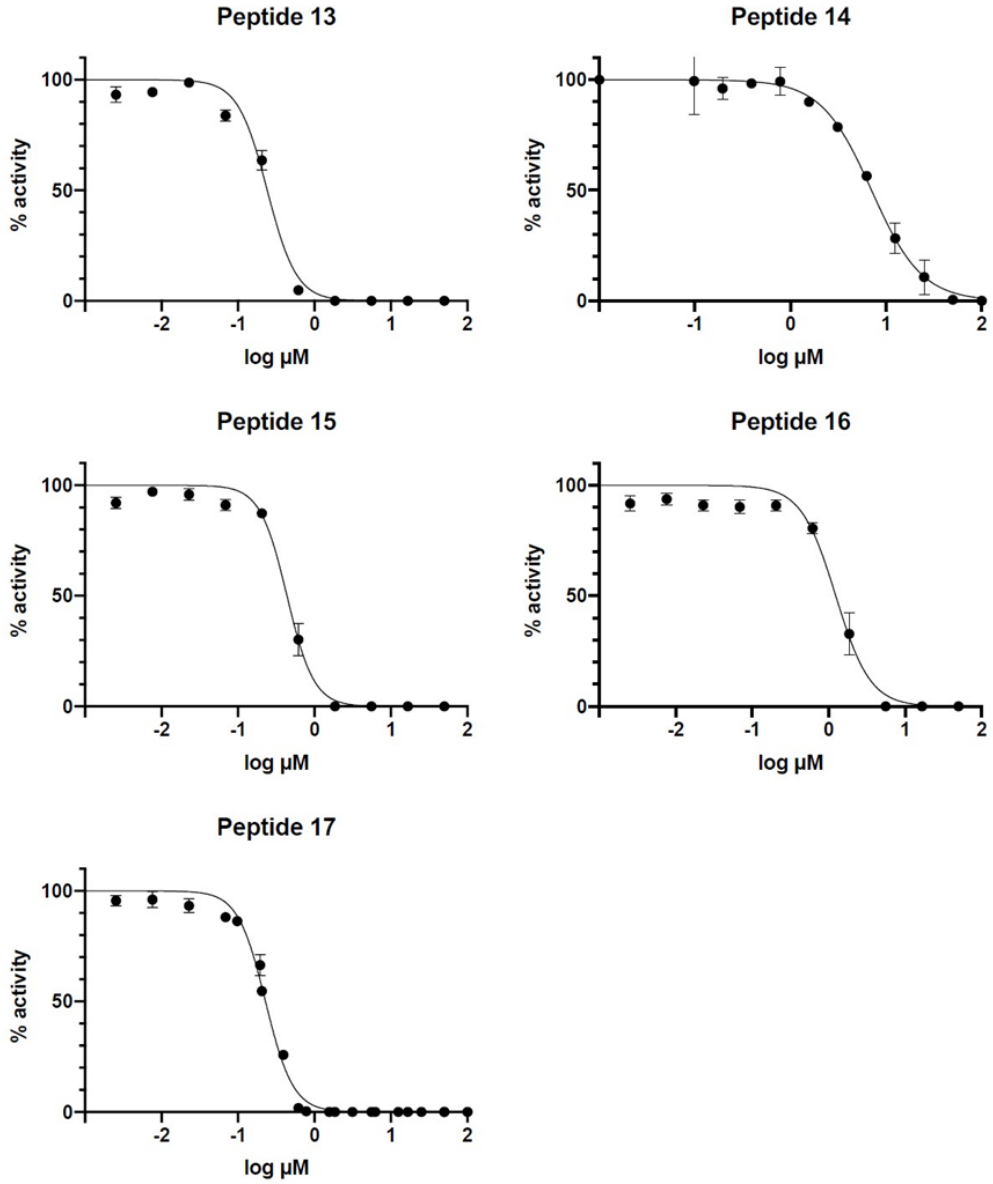

Figure S8. IC_{50} curves for peptides 13-17 against hNNMT. Data is based on triplicate data of at least 10 different concentrations

IC_{50} curves substrate competition

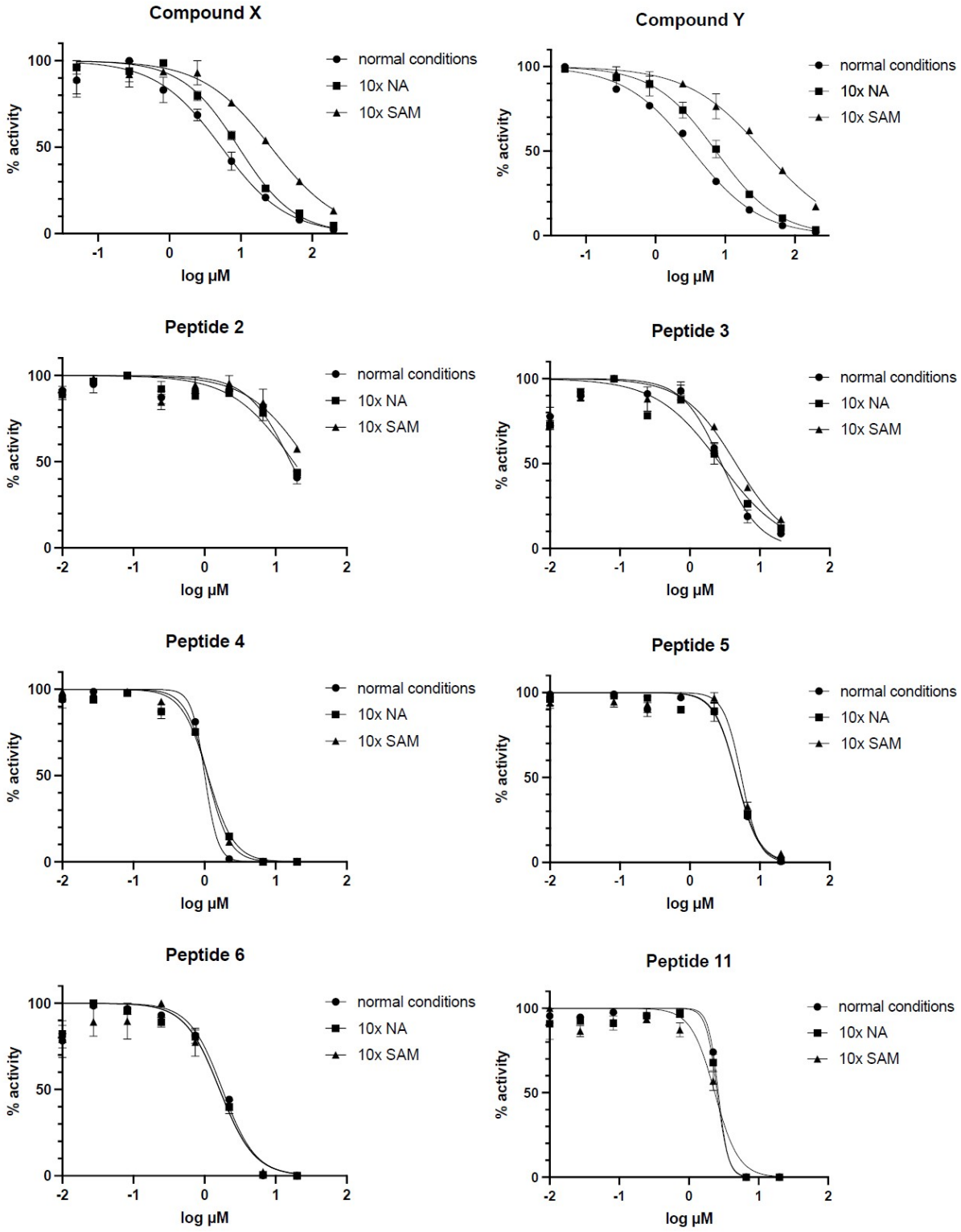

Figure S9. IC_{50} curves for compounds X and Y and peptides 2-6 and 11 against hNNMT. Compounds were tested using normal conditions (substrates at their K_M value), or in the presence of 10-fold higher concentration of either nicotinamide (NA) or Sadenosyl-L-methionine (SAM). Data is based on duplicate data of at 8 different concentrations.

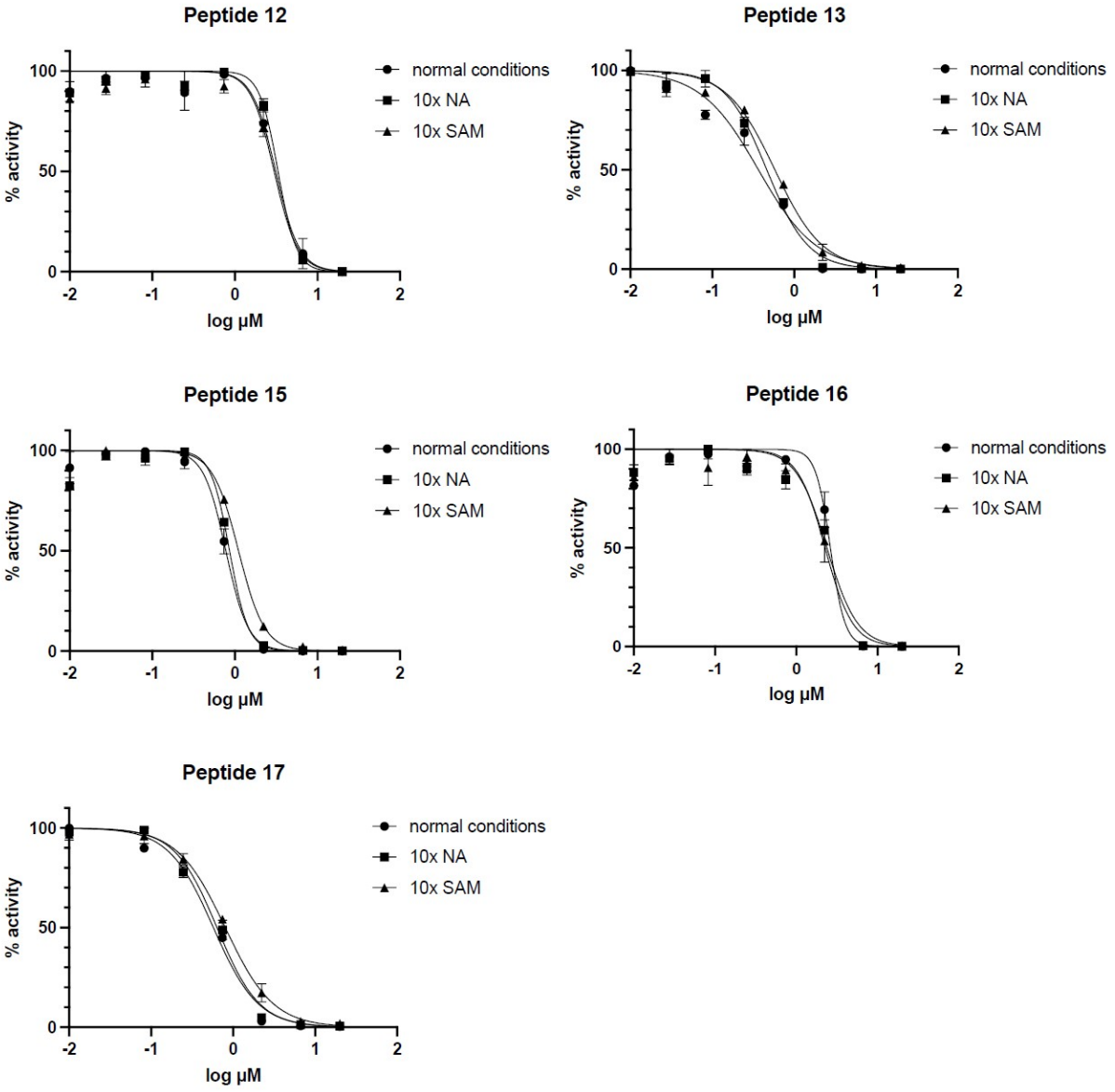

Figure S10. IC_{50} curves for peptides 12-13 and 15-17 against hNNMT. Peptides were tested using normal conditions (substrates at their K_M value), or in the presence of 10-fold higher concentration of either nicotinamide (NA) or S-adenosyl-L-methionine (SAM). Data is based on duplicate data of at 8 different concentrations.

Kinetic analysis mode of inhibition

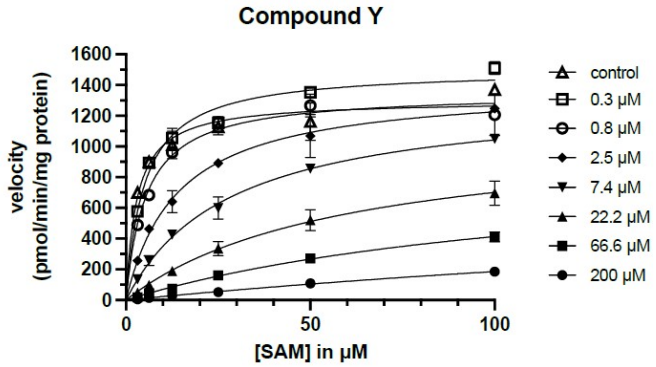

Compound Y	V_{max} (pmol/min/mg)	K_M (µM)
200 µM	853,66 ± 280,87	359,80 ± 144,56
66.6 µM	920,18 ± 95,95	122,58 ± 20,00
22.2 µM	1115,25 ± 107,57	59,12 ± 11,21
7.4 µM	1337,44 ± 47,71	28,24 ± 2,52
2.5 µM	1396,86 ± 50,82	14,00 ± 1,58
0.8 µM	1350,80 ± 43,44	5,42 ± 0,72
0.3 µM	1503,99 ± 40,47	5,03 ± 0,58
control	1299,61 ± 42,57	2,93 ± 0,50

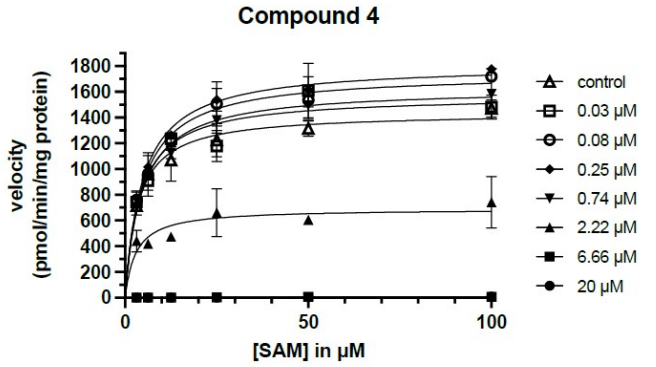

Compound 4	V_{max} (pmol/min/mg)	K_M (µM)
20 µM	-	-
6.66 µM	-	-
2.22 µM	690.79 ± 60.07	2.92 ± 1.34
0.74 µM	1627.80 ± 52.10	4.51 ± 0.64
0.25 µM	1811.27 ± 40.56	4.73 ± 0.46
0.08 µM	1744.78 ± 50.42	4.74 ± 0.59
0.03 µM	1568.55 ± 79.20	4.00 ± 0.93
control	1437.15 ± 55.94	3.41 ± 0.65

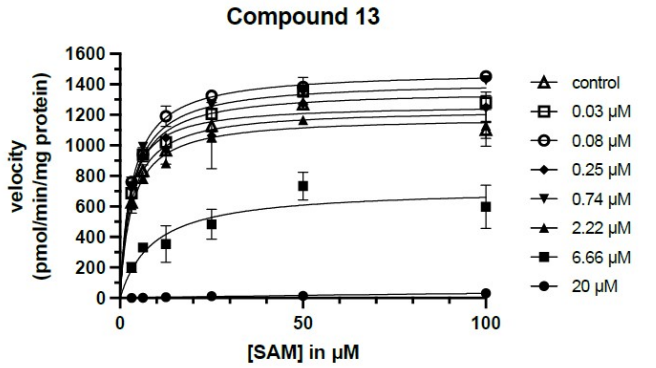

Compound 13	V_{max} (pmol/min/mg)	K_M (µM)
20 µM	-	-
6.66 µM	719,53 ± 76,43	9,08 ± 3.39
2.22 µM	1186,86 ± 32,66	3,23 ± 0.45
0.74 µM	1421,84 ± 47,38	3,29 ± 0.55
0.25 µM	1266,71 ± 47,37	2,41 ± 0.52
0.08 µM	1487,49 ± 18,05	3,22 ± 0.20
0.03 µM	1360,22 ± 32,96	3,11 ± 0.39
control	1237,38 ± 37,19	3,03 ± 0.47

Figure S11. V_{max} and K_M values for NNMT and SAM respectively after treatment of varying concentrations of compound Y, 4 or 13. The change in K_M observed for SAM after treatment with compound Y supports competitive inhibition. The unchanged K_M and changing V_{max} observed for compounds 4 and 13 supports the non-competitive or allosteric mode of inhibition for the cyclic peptides.

Curriculum vitae

Yurui Zhang was born on 28 November 1991 in Datong, China. He started a bachelor's program in pharmaceutic science at Hebei medical University. Since 2011, he started his internship in the laboratory of Prof. Caiqing Yang, studying the preparation of Oleanolic Acid Co-crystals and analysis. After spending two years on bench work, he obtained a bachelor's degree (with distinction). Later, he was enrolled in Peking Union Medical College of TsingHua University in 2014. He conducted his scientific research under Prof. dr. Wenqing Xu, studying in radio protection and radio therapy in vivo and in vitro. In 2017, he was granted his Ph.D. studies from China Scholarship Council (CSC). He subsequently joins the Martin group under the supervision of Prof. dr. Nathaniel I. Martin and Dr. Matthijs J. van Haren. Most of his Ph.D. work is presented in this thesis.

List of Publications

Zhang, Y., van Haren, M.J., Marechal, N., Troffer-Charlier, N., Cura, V., Cavarelli, J., Martin, N.I. A Direct Assay for Measuring Activity and Inhibition of Coactivator Associated Arginine Methyltransferase 1. Biochemistry (Accepted in press)

Zhang, Y., Marechal, N., van Haren, M.J., Troffer-Charlier, N., Cura, V., Cavarelli, J., Martin, N.I. Structural studies provide new insights into the role of lysine acetylation on substrate recognition by CARM1 and inform the design of potent peptidomimetic inhibitors. ChemBioChem. (2021)

van Haren, M.J., Zhang, Y., Thijssen, V., Buijs, N., Gao, Y., Mateuszuk, L., Fedak, F.A., Kij, A., Campagna, R., Sartini, D., Emanuelli, M., Chlopicki, S., Jongkees, S.A.K., Martin, N.I. Macrocyclic Peptides as Allosteric Inhibitors of Nicotinamide N-Methyltransferase (NNMT). RSC Chemical Biology. (2021)

Gao, Y., van Haren, M.J., Buijs, N., Innocenti, P., Zhang, Y., Sartini, D., Campagna, R., Emanuelli, M., Parsons, R.B., Jespers, W., Gutiérrez-de-Terán, H., van Westen, G., Martin, N.I. Potent inhibition of nicotinamide N-methyltransferase by alkene linked bisubstrate mimics bearing electron deficient aromatics. Journal of Medicinal Chemistry. (2021)

Zhang, Y., van Haren, M.J., Martin, N.I. Peptidic transition state analogues as PRMT inhibitors. Methods. (2020)

Zhang, Y., Wang, J., Li, Y., Meng, Y., Zhang, Y., Yang, F., Xu, W. Design and Synthesis a Mitochondria-Targeted Dihydronicotinamide as Radioprotector. Free Radical Biology &Medicine. (2019)

Zhang, Y., Li, Y., Wang, J., Li, Wang, H., Wang, H., Kang, X., Xu, W. Synthesis and characterizaion of a rosmarinic acid derivative that targets mitochondria and protects against radiation-induced damage in vitro. Radiation Research. (2017)

Zhang Y, Wang, J., Li, Y., Wang, F., Yang, F., Xu, W. Synthesis and Radioprotective Activity of Mitochondria Targeted Dihydropyridines. International Journal of Molecular Science. (2017)

Liu, Y., Zhang, C., Zhang, H., Li, M., Yuan, J., Zhang, Y., Zhou, J., Guo, H., Zhao, L., Du, Y., Wang, L., Ren, L. Synthesis and antitumor activity of a novel series of 6-substituted pyrrolo[2,3-d]pyrimidines as potential nonclassical antifolates targeting both thymidylate and purine nucleotide biosynthesis. European Journal of Medicinal Chemistry. (2015)